Scientific Research Publishing

Journal of Mathematical Finance, 2026, 16(4), 247-295
https://www.scirp.org/journal/jmf
ISSN Online: 2162-2442
ISSN Print: 2162-2434

Beyond Valuation Equilibrium: Viability and Persistence in Sustainable Finance

Pascal Stiefenhofer

Department of Economics, Newcastle University Business School, Tyne and Wear, UK
Email: pascal.stiefenhofer@newcastle.ac.uk

How to cite this paper: Stiefenhofer, P. (2026) Beyond Valuation Equilibrium: Viability and Persistence in Sustainable Finance. *Journal of Mathematical Finance*, **16**, 247-295.
https://doi.org/10.4236/jmf.2026.164012

Received: August 18, 2026
Accepted: November 22, 2026
Published: November 25, 2026

Copyright © 2026 by author(s) and Scientific Research Publishing Inc.
This work is licensed under the Creative Commons Attribution-NonCommercial International License (CC BY-NC 4.0).
http://creativecommons.org/licenses/by-nc/4.0/

Open Access

Abstract

Sustainable-finance theory explains how sustainability preferences, ESG demand, and climate risks affect asset prices, expected returns, and capital allocation. Existing models implicitly assume that the financial regime supporting these outcomes remains viable. This paper shows that valuation equilibrium and regime viability are distinct equilibrium concepts. The central result establishes that a sustainable-finance equilibrium may generate sustainability premia and satisfy conventional valuation conditions while remaining incompatible with the conditions required for regime persistence. To characterize this distinction, the analysis derives viability regions and an endogenous transition frontier separating sustainable-growth and fragility regimes. The results imply that sustainability premia, greeniums, and related pricing measures are not sufficient statistics for resilience. Economies with similar valuation outcomes may face markedly different transition risks because viability depends on the broader macro-financial state rather than on equilibrium prices alone. Transition risk is shown to be an endogenous property of equilibrium dynamics determined jointly by frontier location and the direction of state evolution. More generally, the paper extends sustainable finance beyond equilibrium valuation to equilibrium viability and establishes a broader result for systems with endogenous regime switching; equilibrium existence does not guarantee regime persistence.

Keywords

Sustainable Finance, Equilibrium Viability, Regime Persistence, Financial Resilience, Transition Frontier, Endogenous Regime Switching

1. Introduction

A central premise of sustainable finance is that sustainability-related characteris-

tics become incorporated into equilibrium asset prices. Sustainability premia, greeniums, ESG-return differentials, and climate-risk premia are therefore often interpreted as indicators of the strength and persistence of sustainable financial regimes. Yet valuation and persistence are conceptually distinct.

Two economies may exhibit identical sustainability premia while differing substantially in liquidity conditions, information quality, investor participation, systemic stress, and climate-risk salience. One regime may remain resilient whereas the other may be approaching collapse. Similarly, a sustainable-finance equilibrium may generate positive sustainability premia and internally consistent expected-return relations while simultaneously evolving toward conditions incompatible with its continued existence. Valuation therefore does not identify viability.

This observation raises a fundamental equilibrium problem. Under what conditions does a sustainable-finance equilibrium remain compatible with the continued existence of the regime supporting it?

Existing sustainable-finance theories explain how sustainability characteristics are incorporated into prices, expected returns, portfolio allocations, ownership structures, and financing conditions [1]-[7]. Existing climate-finance models explain how climate risks affect asset prices, investor behavior, and portfolio allocation [8]-[14]. Existing macro-financial theories explain how financial systems become resilient or fragile through liquidity shortages, leverage cycles, balance-sheet amplification, funding constraints, and systemic-risk externalities [15]-[21].

Related general-equilibrium work with incomplete financial markets shows that production, financing, and corporate objectives can be jointly determined when markets are incomplete, including environments with endogenous production capacity and nonsmooth production technologies [22]-[25]. This reinforces the broader point that an internally coherent valuation or allocation system need not exhaust the economically relevant state description. At the individual-investor level, recent neurofinance work likewise models valuation as state dependent and shows that financially equivalent dynamics can be associated with different subjective temporal trajectories [26].

These literatures address closely related questions but focus on different objects. Sustainable-finance theory studies valuation. Climate-finance theory studies climate-risk pricing. Macro-financial theory studies fragility and instability. None provides an equilibrium concept governing whether the state supporting a sustainable-finance equilibrium remains dynamically admissible over time.

The central contribution of this paper is therefore not another channel through which sustainability affects equilibrium prices. Instead, the paper introduces a distinct equilibrium object.

We define *viability equilibrium* as an equilibrium condition governing whether a sustainable-finance regime remains admissible under the endogenous evolution of the macro-financial state. Whereas valuation equilibrium determines whether prices, expected returns, portfolio allocations, and financing conditions are mu-

tually consistent, viability equilibrium determines whether the regime supporting those outcomes remains capable of persisting.

The central result of the paper is

$$\text{Valuation Equilibrium} \not\Rightarrow \text{Viability Equilibrium}.$$

A sustainable-finance equilibrium may therefore satisfy the valuation system, generate sustainability premia, greeniums, and internally consistent expected-return relations while simultaneously approaching a state incompatible with regime persistence. Conversely, economies exhibiting similar sustainability premia may possess substantially different probabilities of regime survival because they occupy different locations in a broader macro-financial state space. Equilibrium prices are therefore not, in general, sufficient statistics for resilience, fragility, or transition risk.

To formalize this distinction, we develop a sustainable macro-financial framework in which viability is determined jointly by sustainable-investment demand, investor participation, information quality, market liquidity, systemic financial stress, and climate concern. These variables correspond to observable quantities studied extensively throughout the sustainable-finance, climate-finance, and financial-stability literatures and collectively define an endogenous admissibility structure governing regime persistence.

The resulting state-space geometry partitions the economy into viability and fragility regions separated by endogenous transition frontiers. The location of an economy within this geometry determines whether a valuation equilibrium is also compatible with continued regime persistence.

The paper contributes to several strands of literature. First, it contributes to sustainable-finance theory by extending the analysis of sustainability beyond equilibrium valuation. Existing models explain how sustainability characteristics affect prices, expected returns, portfolio allocations, and ownership structures [1] [3] [5]-[7]. The present framework studies whether the resulting regime remains capable of persisting. Second, it contributes to the empirical and institutional literature on sustainable investing. Studies document sustainability premia, greeniums, ownership effects, capital-flow effects, financing advantages, and emerging AI-enabled sustainable trading strategies associated with sustainable-investment demand [27]-[37]. The framework developed here implies that such valuation outcomes need not uniquely determine the resilience of the underlying sustainable-finance regime. Third, the paper contributes to climate finance. Recent research demonstrates that climate risks influence investor expectations, portfolio allocations, hedging behavior, and equilibrium asset prices [8]-[14]. The present framework complements this literature by studying the conditions under which climate-related financial regimes remain viable. Fourth, the paper contributes to macro-financial theory. A large literature studies liquidity shortages, funding constraints, leverage cycles, amplification mechanisms, and systemic-risk externalities [15]-[21]. The viability framework links these sources of fragility to the per-

sistence of sustainable-finance equilibria and provides a formal state-space representation of regime survival.

More broadly, the paper identifies a distinction between valuation consistency and regime persistence. Valuation equilibrium and viability equilibrium coincide only under special conditions. In general, sustainability can be correctly priced without the resulting regime being viable. Sustainable finance therefore requires not only a theory of valuation but also a theory of persistence.

The remainder of the paper is organized as follows. Section 2 develops the sustainable macro-financial state-space framework and the associated regime dynamics. Section 3 defines viability equilibrium and derives the principal theoretical results. Section 4 examines policy-modified viability regions and state-dependent transition frontiers. Section 5 relates the findings to the broader sustainable-finance, climate-finance, macro-financial, and financial-stability literatures. Section 6 concludes. Section 6 is an appendix.

2. A Sustainable Macro-Financial Switching Framework

This section develops a sustainable macro-financial framework in which asset pricing, regime viability, and endogenous regime switching are jointly determined. The model is constructed in five steps. First, a sustainable-investing equilibrium determines asset prices and expected returns conditional on a prevailing financial regime. Second, the macro-financial environment is endogenized through a dynamic state system governing ESG demand, investor participation, information quality, market liquidity, systemic financial stress, and climate concern. Third, these state variables jointly determine regime viability. Fourth, endogenous transitions arise when the economy crosses critical viability boundaries. Finally, an admissibility structure links valuation outcomes to regime persistence. Together, these elements embed sustainable-finance valuation within a broader macro-financial system with endogenous regime switching.

2.1. Sustainable-Finance Pricing Equilibrium

The first component of the framework determines equilibrium expected returns conditional on a given macro-financial regime. Following [5] [6], investors derive utility from both financial wealth and the sustainability characteristics of their portfolios.

Consider an economy with N risky assets and a risk-free asset. At each instant, the economy operates in one of two macro-financial regimes,

$$\sigma(t) \in \{G, F\}, \tag{1}$$

where G denotes the sustainable-growth regime and F denotes the financial-fragility regime. Throughout this subsection, σ is taken as given. Endogenous regime determination is introduced in Section 2.5. Conditional on regime σ, excess returns satisfy

$$\tilde{r}(t) = \mu_\sigma(t) + \tilde{\varepsilon}_\sigma(t), \quad \tilde{\varepsilon}_\sigma(t) \sim N(0, \Sigma_\sigma), \tag{2}$$

where $\mu_\sigma(t) \in \mathbb{R}^N$ denotes the vector of expected excess returns and

$$\Sigma_\sigma = \Sigma_\sigma' \succ 0. \tag{3}$$

Each risky asset possesses an observable sustainability characteristic. Let

$$g = (g_1, \cdots, g_N)' \in \mathbb{R}^N, \ g \neq 0, \tag{4}$$

denote the vector of ESG characteristics, where larger values correspond to greener assets and smaller values to browner assets. Let $w_m \in \mathbb{R}^N$ denote the market portfolio of risky assets. We impose the normalization

$$\iota' w_m = 1, \tag{5}$$

where ι denotes the N-vector of ones. Following [5], sustainability characteristics are measured relative to the market portfolio through

$$w_m' g = 0. \tag{6}$$

Condition (6) removes the aggregate market component of sustainability exposure and isolates the purely cross-sectional ESG dimension. Investors derive nonpecuniary utility from holding assets with desirable sustainability characteristics. Let $X_i(t) \in \mathbb{R}^N$ denote the risky-asset holdings of investor i. The associated sustainability benefit is

$$b_i(t)' X_i(t) = d_i(t) g' X_i(t), \tag{7}$$

where $d_i(t) \geq 0$ measures investor i's preference for sustainability. Define the wealth-weighted aggregate ESG preference

$$\bar{d}(t) = \int \omega_i(t) d_i(t) \mathrm{d}i, \quad \omega_i(t) \geq 0, \quad \int \omega_i(t) \mathrm{d}i = 1, \tag{8}$$

where $\omega_i(t)$ denotes investor wealth shares. All investors share a common coefficient of relative risk aversion $a > 0$. Conditional on regime σ, market clearing implies the sustainable-investing equilibrium of [5] [6]. Expected returns satisfy

$$\mu_\sigma^{ESG}(t) = \mu_{m,\sigma}(t) \beta_{m,\sigma} - \frac{\bar{d}(t)}{a} g, \tag{9}$$

where

$$\mu_{m,\sigma}(t) = w_m' \mu_\sigma^{ESG}(t), \quad \beta_{m,\sigma} = \frac{\Sigma_\sigma w_m}{w_m' \Sigma_\sigma w_m}. \tag{10}$$

Equation (9) decomposes expected returns into a systematic-risk component, $\mu_{m,\sigma}\beta_{m,\sigma}$, and a sustainability-demand component, $-(\bar{d}/a)g$. An increase in $\bar{d}(t)$ lowers the expected returns of greener assets and raises the expected returns of browner assets. The sustainable-finance environment is additionally affected by aggregate climate concern. Let $c(t) \geq 0$ denote the climate-concern index and let $\psi_\sigma \in \mathbb{R}^N$ denote the regime-specific climate-risk loading vector. The pricing equilibrium is therefore extended to

$$\mu_{\sigma(t)}(t) = \mu_{m,\sigma(t)}(t)\beta_{m,\sigma(t)} - \frac{\bar{d}(t)}{a}g + \pi_{c,\sigma(t)}c(t)\psi_{\sigma(t)}, \tag{11}$$

where $\pi_{c,\sigma(t)}$ measures the sensitivity of expected returns to aggregate climate concern. Equation (11) defines the valuation equilibrium used throughout the remainder of the paper. In particular, the equilibrium-return system (11) will be evaluated both along endogenous state trajectories and at frozen-regime equilibria. To isolate the sustainability-demand component of equilibrium pricing without confounding it with market or climate-risk exposure, define

$$A_\sigma = \begin{pmatrix} \beta_{m,\sigma} & \psi_\sigma \end{pmatrix}$$

and assume that A_σ has full column rank and that $g \notin \operatorname{span}(A_\sigma)$. Let

$$M_\sigma = I - A_\sigma \left(A_\sigma' A_\sigma\right)^{-1} A_\sigma' \tag{12}$$

be the orthogonal projector onto the complement of the span of market and climate-risk loadings. For any non-zero normalization constant $\gamma_{g,\sigma}$, define the regime-specific ESG factor portfolio

$$w_{g,\sigma} = \gamma_{g,\sigma} \frac{M_\sigma g}{g' M_\sigma g}. \tag{13}$$

Then

$$w_{g,\sigma}'\beta_{m,\sigma} = 0, \quad w_{g,\sigma}'\psi_\sigma = 0, \quad w_{g,\sigma}'g = \gamma_{g,\sigma}. \tag{14}$$

Projecting the extended pricing relation (11) onto (13) therefore gives

$$\mu_{g,\sigma}(t) := w_{g,\sigma}'\mu_\sigma(t) = -\frac{\bar{d}(t)}{a}\gamma_{g,\sigma}. \tag{15}$$

Equation (15) is the model's greenium measure: it isolates the valuation effect of ESG demand after removing the market and climate-risk components. The normalization $\gamma_{g,\sigma} = 1$ gives a unit-ESG-exposure factor; retaining $\gamma_{g,\sigma}$ makes explicit that the numerical magnitude of the portfolio return depends on the chosen factor normalization.

The full expected-return vector, however, is not a function of $\bar{d}$ alone. Conditional on the active regime it depends directly on $\bar{d}$ and c through Equation (11), while the remaining state variables affect valuation indirectly through the endogenous regime-selection map. In particular, if $u = (\bar{d}, \lambda, z, q, \ell, c)$ and σ^- denotes the left-limit regime, then the valuation system can be written as

$$\mu = \mathcal{M}\left(\bar{d}, c, \mathcal{S}\left(u, \sigma^-\right)\right), \tag{16}$$

where $\mathcal{S}$ is the hysteretic switching map defined below. Thus the full state vector jointly determines realized valuation through direct valuation channels $(\bar{d}, c)$ and the regime-selection channel, without imposing the incorrect claim that every state variable enters the pricing equation directly.

The pricing equilibrium developed in this subsection determines equilibrium valuation conditional on a regime. However, Equations (9)-(16) do not determine whether the regime generating that valuation equilibrium can persist. Regime

persistence depends on the evolution of the macro-financial environment. We therefore next introduce the endogenous state dynamics governing ESG demand, investor participation, systemic stress, information quality, market liquidity, and climate concern. The distinction between valuation equilibrium and regime persistence will ultimately underpin the paper's central result that equilibrium existence need not imply viability equilibrium.

2.2. Economic Environment

The sustainable-investing equilibrium developed above determines asset prices conditional on the prevailing economic environment. We now endogenize that environment. The key observation is that sustainable-finance valuation depends on more than ESG demand alone. The persistence of a sustainable-finance regime also depends on investor participation, information quality, market liquidity, financial conditions, and climate concern. These variables jointly determine both equilibrium valuation and regime viability. Define the macro-financial state vector

$$u = \left(\bar{d}, \lambda, q, \ell, z, c\right),$$

where $\bar{d}$ denotes aggregate ESG demand, λ the participation of ESG-oriented investors, q ESG-information quality, ℓ green-market liquidity, z systemic financial stress, and c climate concern.

Aggregate ESG demand $\bar{d}$ captures the demand channel through which sustainability preferences affect asset prices [1] [5] [7]. Participation λ measures the breadth and persistence of sustainable-investment activity [28] [31] [32] [35]. Information quality q captures the reliability of ESG disclosures, ratings, and sustainability information available to investors [34] [38] [39]. Liquidity ℓ measures the ability of sustainable-asset markets to absorb portfolio rebalancing without destabilizing prices [15] [16]. Systemic stress z captures aggregate macro-financial fragility [17] [18] [20]. Climate concern c measures the salience of climate-related risks in investor beliefs and portfolio decisions [8] [9] [13] [40]. The state vector u is not an auxiliary collection of state variables. It is the object that determines regime viability. Asset prices determine how sustainability is valued; the state vector determines whether the regime supporting those valuations can persist. The next subsection specifies the dynamics of u and thereby links valuation, viability, and endogenous regime transitions within a unified state-space framework.

2.3. Macro-Financial State Dynamics

The variables introduced in the previous subsection jointly define the macro-financial state of the economy. Let

$$u(t) = \left(\bar{d}(t), \lambda(t), z(t), q(t), \ell(t), c(t)\right) \in D, \tag{17}$$

denote the state vector, where $\bar{d}$ is aggregate ESG demand, λ the wealth share

of ESG-oriented investors, z systemic financial stress, q ESG-information quality, ℓ green-market liquidity, and c aggregate climate concern. The admissible state space is

$$D=\left\{\left(\bar{d},\lambda,z,q,\ell,c\right)\in\mathbb{R}^6:\bar{d}\geq 0,\lambda\in\left[0,1\right],z\geq 0,q\in\left[0,1\right],\ell\in\left[0,1\right],c\geq 0\right\}. \quad (18)$$

The constraints in (18) reflect economic feasibility. ESG demand, systemic stress, and climate concern are nonnegative, while participation, information quality, and liquidity are bounded proportions. The evolution of the economy is governed by a state-dependent dynamical system on D. Conditional on the active regime $\sigma(t)\in\{G,F\}$, the state evolves according to

$$\dot{u}(t)=F_{\sigma(t)}\left(u(t)\right), \quad (19)$$

where

$$F_\sigma(u)=\begin{pmatrix}\rho_\sigma\left(\bar{d}_\sigma^*-\bar{d}\right)-\rho_{\sigma z}z+\rho_{\sigma q}q\\ \lambda(1-\lambda)\left[\Pi_\sigma\left(\bar{d},q,\ell\right)-\Gamma_\sigma z\right]\\ -\kappa_\sigma z+\eta_{\sigma d}\bar{d}+\eta_{\sigma\lambda}\lambda+\eta_{\sigma q}q-\omega_\sigma(1-\ell)\\ r_\sigma\left(\bar{q}_\sigma-q\right)-\chi_\sigma z\\ s_\sigma\left(\bar{\ell}_\sigma-\ell\right)-\nu_\sigma z+\tau_\sigma\lambda\\ m_\sigma\left(\bar{c}_\sigma-c\right)+\xi_\sigma z\end{pmatrix}. \quad (20)$$

The component formula in Equation (20) is the unconstrained drift. Because D contains economically meaningful boundaries, the actual deterministic state law is its tangent-cone projection. For $u\in D$ and $v\in\mathbb{R}^6$, let

$$\mathcal{T}_D(u,v):=\arg\min_{w\in T_D(u)}\|w-v\|, \quad (21)$$

where $T_D(u)$ is the Bouligand tangent cone of D at u. Define

$$\hat{F}_\sigma(u):=\mathcal{T}_D\left(u,F_\sigma(u)\right),\quad \dot{u}=\hat{F}_{\sigma(t)}(u). \quad (22)$$

In the interior D°, $\hat{F}_\sigma=F_\sigma$, so all interior comparative statics and frozen-equilibrium calculations below are unchanged. At a lower boundary, the projection replaces a negative outward component by zero; at an upper boundary of λ,q, or ℓ, it replaces a positive outward component by zero. This convention is economically equivalent to a hard feasibility constraint and avoids imposing parameter restrictions that would otherwise have to hold for arbitrarily large values of the unbounded stress state z.

Proposition 1 (Positive invariance of the admissible state space) *Suppose F_σ is locally Lipschitz on a neighbourhood of D for each $\sigma\in\{G,F\}$. Then every Carathéodory solution of (22) with $u(0)\in D$ satisfies $u(t)\in D$ for all times for which the solution exists.*

Proof. By construction, $\hat{F}_\sigma(u)\in T_D(u)$ for every $u\in D$. Hence at every active constraint the projected velocity is tangent to or points into D. The standard viability/Nagumo tangency condition therefore holds pointwise. Since D is closed and convex and the projected field is measurable in time and locally

bounded, a solution starting in D cannot cross any face of ∂D with an outward velocity. Thus D is positively invariant.

For notational economy, subsequent formulas involving Lie derivatives use F_σ on D°; whenever a trajectory reaches ∂D, the same formula is understood with $\hat{F}_\sigma$ from (22).

Equation (20) defines a regime-dependent macro-financial feedback system linking ESG demand, investor participation, information quality, market liquidity, systemic financial stress, and climate concern. The same variables that determine equilibrium valuation therefore govern the evolution of regime viability. Persistence is thus an endogenous property of the state system rather than an imposed assumption.

The first equation describes adjustment of aggregate ESG demand toward the regime-specific benchmark $\bar{d}_\sigma^*$, with demand strengthened by information quality and weakened by systemic stress. The second equation governs the evolution of ESG participation through a logistic mechanism in which investor entry and exit depend on the relative attractiveness of sustainable investment. The remaining equations determine the joint dynamics of financial stress, information quality, market liquidity, and climate concern. A central role is played by the participation equation. Let

$$D_\Pi = \left\{\left(\bar{d}, q, \ell\right) : \bar{d} \geq 0, q \in [0,1], \ell \in [0,1]\right\},$$

and define

$$\Pi_\sigma : D_\Pi \to \mathbb{R}$$

as the regime-dependent attractiveness of ESG-oriented investment. The function Π_σ summarizes the forces that encourage capital reallocation toward ESG-oriented investment, while $\Gamma_\sigma z$ captures the reduction in participation generated by systemic financial stress. To make the valuation and participation primitives fully explicit, the baseline specification used for the analytical examples and numerical illustration is

$$\Pi_\sigma\left(\bar{d}, q, \ell\right) = \alpha_{\sigma 0} + \alpha_{\sigma d}\bar{d} + \alpha_{\sigma q} q + \alpha_{\sigma \ell}\ell, \quad \alpha_{\sigma d}, \alpha_{\sigma q}, \alpha_{\sigma \ell} \geq 0. \tag{23}$$

The general results require only $\Pi_\sigma \in C^1\left(D_\Pi\right)$ and

$$\frac{\partial \Pi_\sigma}{\partial \bar{d}} \geq 0, \quad \frac{\partial \Pi_\sigma}{\partial q} \geq 0, \quad \frac{\partial \Pi_\sigma}{\partial \ell} \geq 0. \tag{24}$$

Hence stronger ESG demand, higher-quality information, and greater market liquidity weakly increase ESG-investment attractiveness. Equation (23) also makes clear exactly which state variables enter the participation primitive: $\left(\bar{d}, q, \ell, z\right)$ enters directly through $\Pi_\sigma - \Gamma_\sigma z$, whereas λ enters through the logistic term and the other state variables operate through the coupled state dynamics. Using (20), the participation component of the vector field is

$$F_\sigma^\lambda(u) = \lambda(1-\lambda)\left[\Pi_\sigma\left(\bar{d}, q, \ell\right) - \Gamma_\sigma z\right]. \tag{25}$$

The logistic term $\lambda(1-\lambda)$ ensures that $\lambda \in [0,1]$, while $\Pi_\sigma(\bar{d}, q, \ell) - \Gamma_\sigma z$ determines whether ESG participation expands or contracts. Differentiating (25) and using (24) yields

$$\frac{\partial F_\sigma^\lambda}{\partial \bar{d}} = \lambda(1-\lambda)\frac{\partial \Pi_\sigma}{\partial \bar{d}} \geq 0, \tag{26}$$

$$\frac{\partial F_\sigma^\lambda}{\partial q} = \lambda(1-\lambda)\frac{\partial \Pi_\sigma}{\partial q} \geq 0, \tag{27}$$

$$\frac{\partial F_\sigma^\lambda}{\partial \ell} = \lambda(1-\lambda)\frac{\partial \Pi_\sigma}{\partial \ell} \geq 0, \tag{28}$$

and

$$\frac{\partial F_\sigma^\lambda}{\partial z} = -\lambda(1-\lambda)\Gamma_\sigma \leq 0. \tag{29}$$

Equations (26)-(29) show that ESG participation is reinforced by demand, information quality, and liquidity, and weakened by systemic financial stress. The participation channel therefore links current valuation conditions to the future composition of investors. The state system (19)-(20) determines the evolution of the macro-financial environment. Regime selection, however, requires a state-dependent measure of resilience and fragility. We therefore next construct the sustainability-fragility geometry that maps the state vector (17) into an endogenous regime-selection mechanism.

2.4. Sustainability-Fragility Geometry

The state system (19)-(20) evolves in the six-dimensional state space D. Regime selection, however, depends on a lower-dimensional summary of the macro-financial environment. We therefore introduce a scalar index that maps the state vector (17) into a one-dimensional measure of resilience and fragility.

Definition 1 (Sustainability-fragility index)

Define

$$\Xi : D \to \mathbb{R}, \quad \Xi(u) = z + \vartheta(1-q) + \upsilon(1-\ell) - \rho_d \bar{d} - \rho_\lambda \lambda + \rho_c c, \tag{30}$$

where

$$\vartheta, \upsilon, \rho_d, \rho_\lambda, \rho_c > 0.$$

The mapping (30) projects the multidimensional state vector (17) onto a single fragility coordinate. Systemic stress, informational opacity, illiquidity, and climate concern increase Ξ, whereas ESG demand and ESG-investor participation reduce it. Consequently, larger values of Ξ correspond to more fragile macro-financial conditions, while smaller values correspond to greater resilience. The gradient of the fragility index is

$$\nabla \Xi(u) = (-\rho_d, -\rho_\lambda, 1, -\vartheta, -\upsilon, \rho_c). \tag{31}$$

Equation (31) implies

$$\frac{\partial \Xi}{\partial z} = 1, \quad \frac{\partial \Xi}{\partial c} = \rho_c > 0, \tag{32}$$

and

$$\frac{\partial \Xi}{\partial \bar{d}} = -\rho_d, \quad \frac{\partial \Xi}{\partial \lambda} = -\rho_\lambda, \quad \frac{\partial \Xi}{\partial q} = -\vartheta, \quad \frac{\partial \Xi}{\partial \ell} = -\upsilon. \tag{33}$$

Equation (32) and Equation (33) show that larger values of Ξ correspond to greater macro-financial fragility. The mapping (30) therefore reduces the six-dimensional state vector (17) to a one-dimensional fragility coordinate. Regime selection depends on the position of the economy in this induced fragility space rather than directly on the individual state variables. Position alone, however, is not sufficient to characterize regime dynamics. Regime transitions also depend on the direction in which the economy moves through fragility space. We therefore study the evolution of Ξ along trajectories of the state system (19).

Definition 2 (Switching pressure)

For each regime $\sigma \in \{G, F\}$, define

$$L_{F_\sigma}\Xi(u) = \nabla\Xi(u)^\top F_\sigma(u), \tag{34}$$

where F_σ is the frozen-regime vector field defined in Equation (20).

Substituting Equation (31) and Equation (20) into Equation (34) yields

$$\begin{aligned} L_{F_\sigma}\Xi(u) = &-\rho_d F_\sigma^d(u) - \rho_\lambda F_\sigma^\lambda(u) + F_\sigma^z(u) \\ &- \vartheta F_\sigma^q(u) - \upsilon F_\sigma^\ell(u) + \rho_c F_\sigma^c(u). \end{aligned} \tag{35}$$

Equation (35) is the fundamental object governing regime transitions. It determines whether the economy moves toward greater resilience or greater fragility. Specifically,

$$L_{F_\sigma}\Xi(u) < 0 \tag{36}$$

implies movement toward greater resilience, whereas

$$L_{F_\sigma}\Xi(u) > 0 \tag{37}$$

implies movement toward greater fragility. Together, (30), (36), and (37) provide a geometric representation of regime viability. The fragility coordinate Ξ determines the position of the economy in fragility space, while the switching pressure $L_{F_\sigma}\Xi$ determines its direction of motion. Regime selection is obtained by combining these two objects with a state-dependent switching rule. We therefore next construct the hysteretic mechanism that converts continuous state evolution into discrete macro-financial regime transitions.

2.5. Hysteretic Regime Switching

The sustainability-fragility geometry developed in Section 2.4 determines how resilience and fragility evolve across the state space. We now use this geometry to construct the endogenous switching mechanism that governs transitions between sustainable-growth and financial-fragility states. Regime transitions occur when the fragility index Ξ crosses critical thresholds. To prevent spurious reversals

generated by small local fluctuations, switching is assumed to exhibit hysteresis. Define two switching thresholds

$$0 < \bar{\zeta}_- < \bar{\zeta}_+. \tag{38}$$

Equation (38) creates a nonempty interval separating sustainable-growth states from financial-fragility states. The associated switching manifolds are

$$\mathcal{S}_- = \{u \in D : \Xi(u) = \bar{\zeta}_-\}, \quad \mathcal{S}_+ = \{u \in D : \Xi(u) = \bar{\zeta}_+\}, \tag{39}$$

where Ξ is defined in Equation (30). The lower manifold $\mathcal{S}_-$ forms the recovery boundary beyond which the economy enters the sustainable-growth region, whereas the upper manifold $\mathcal{S}_+$ forms the fragility boundary beyond which the financial-fragility state becomes active. These manifolds partition the state space into three regions. The sustainable-growth region is

$$\mathcal{D}_G = \{u \in D : \Xi(u) \le \bar{\zeta}_-\}, \tag{40}$$

the financial-fragility region is

$$\mathcal{D}_F = \{u \in D : \Xi(u) \ge \bar{\zeta}_+\}, \tag{41}$$

and the hysteresis region is

$$\mathcal{H} = \{u \in D : \bar{\zeta}_- < \Xi(u) < \bar{\zeta}_+\}. \tag{42}$$

The region $\mathcal{H}$ defined by Equation (42) does not constitute a separate regime. Instead, it is a continuation region in which the currently active state persists until one of the switching boundaries is crossed. The presence of the hysteresis region introduces path dependence. The active state therefore depends not only on the current position of the economy in the state space but also on the history through which that position was attained. The regime-selection rule is

$$\sigma(t) = \begin{cases} F, & \Xi(u(t)) \ge \bar{\zeta}_+, \\ G, & \Xi(u(t)) \le \bar{\zeta}_-, \\ \sigma(t^-), & \bar{\zeta}_- < \Xi(u(t)) < \bar{\zeta}_+. \end{cases} \tag{43}$$

The forced-selection regions $\mathcal{D}_G$ and $\mathcal{D}_F$ must be distinguished from the continuation sets of an already active regime. Under hysteresis, an active growth regime continues throughout the band until the upper boundary is reached, whereas an active fragility regime continues until the lower recovery boundary is reached. Accordingly define

$$\mathcal{C}_G = \{u \in D : \Xi(u) < \bar{\zeta}_+\}, \quad \mathcal{C}_F = \{u \in D : \Xi(u) > \bar{\zeta}_-\}. \tag{44}$$

Thus $\mathcal{H} \subset \mathcal{C}_G \cap \mathcal{C}_F$: within the continuation band current state information alone does not identify the regime; history does. At $\mathcal{S}_+$ the switching rule assigns F, so G ceases to be compatible, and at $\mathcal{S}_-$ the switching rule assigns G, so F ceases to be compatible. These strict continuation inequalities exactly match the weak inequalities in Equation (43).

Equation (43) maps the continuous state dynamics (19) into discrete regime

transitions. The hysteresis band (38) ensures that arbitrarily small perturbations cannot generate immediate reversals. Transitions therefore occur only when fragility accumulates sufficiently to cross one of the switching boundaries (39). Combining the continuous state dynamics (19) with the switching rule (43) generates a hybrid dynamical system consisting of continuous within-regime evolution and discrete endogenous transitions across the switching manifolds.

The switching mechanism is central to the analysis because it separates equilibrium existence from regime persistence. A stationary equilibrium may satisfy the local equilibrium conditions associated with a given vector field while lying outside the region in which that state can remain sustainable under the endogenous switching dynamics. The resulting distinction between equilibrium existence and regime compatibility provides the foundation for the viability analysis developed below. It ultimately leads to the paper's central result that valuation equilibrium and viability equilibrium are distinct equilibrium concepts.

2.6. Frozen Equilibria, Compatibility, and Local Persistence

Definition 3 (Frozen-regime equilibrium) *For* $\sigma \in \{G, F\}$, *an interior frozen-regime equilibrium is a state*

$$u_\sigma^* \in D^\circ, \quad F_\sigma\left(u_\sigma^*\right) = 0. \tag{45}$$

Boundary equilibria are defined analogously using $\hat{F}_\sigma\left(u_\sigma^*\right) = 0$.

Let

$$J_\sigma(u) = DF_\sigma(u) \tag{46}$$

denote the Jacobian of the interior frozen-regime field.

Proposition 2 (Local uniqueness of a frozen-regime equilibrium) *Suppose* F_σ *is continuously differentiable on a neighbourhood of an interior state* u_σ^* *satisfying Equation* (45). *If*

$$\det J_\sigma\left(u_\sigma^*\right) \neq 0, \tag{47}$$

then u_σ^* is an isolated, locally unique root of $F_\sigma(u) = 0$.

Proof. The derivative $DF_\sigma\left(u_\sigma^*\right) = J_\sigma\left(u_\sigma^*\right)$ is nonsingular. The inverse function theorem therefore gives neighbourhoods U of u_σ^* and V of zero such that $F_\sigma : U \to V$ is a diffeomorphism. Hence $F_\sigma(u) = 0$ has exactly one solution in U, namely u_σ^*.

Proposition 2 is deliberately a local uniqueness result: it does not assert that a root exists. Existence may be established by standard fixed-point or degree arguments under additional global conditions; for the separation result it is enough, and more transparent, to exhibit an explicit root that is incompatible with its frozen regime.

Example 1 (An incompatible frozen growth equilibrium) *Consider the affine attractiveness function in Equation* (23) *and set, for regime* G,

$$\rho_G = r_G = s_G = m_G = \Gamma_G = 1, \quad \rho_{Gz} = \rho_{Gq} = \chi_G = \nu_G = \tau_G = \xi_G = 0.2,$$

$$\kappa_G = 0.2, \quad \eta_{Gd} = \eta_{G\lambda} = \eta_{Gq} = \omega_G = 0.2, \quad \left(\bar{d}_G^*, \bar{q}_G, \bar{\ell}_G, \bar{c}_G\right) = (0.6, 0.7, 0.6, 0.3),$$

and

$$\Pi_G\left(\bar{d}, q, \ell\right) = 0.7 + 0.2\bar{d} + 0.2q + 0.2\ell.$$

Then

$$u_G^* = (0.5, 0.5, 1, 0.5, 0.5, 0.5)$$

(in the order $\left(\bar{d}, \lambda, z, q, \ell, c\right)$) satisfies all six equations $F_G\left(u_G^*\right) = 0$. Direct differentiation gives

$$\det J_G\left(u_G^*\right) = 0.0644 \neq 0,$$

so the root is locally unique by Proposition 2. Now choose

$$\vartheta = \upsilon = \rho_d = \rho_\lambda = \rho_c = 0.2, \quad \left(\bar{\zeta}_-, \bar{\zeta}_+\right) = (0.4, 0.8).$$

Then

$$\Xi\left(u_G^*\right) = 1 + 0.2(0.5) + 0.2(0.5) - 0.2(0.5) - 0.2(0.5) + 0.2(0.5) = 1.1 > 0.8 = \bar{\zeta}_+.$$

Thus u_G^* is a genuine, locally unique frozen G equilibrium, but the full hysteretic rule selects F at that same state. This provides a constructive witness that frozen equilibrium existence does not imply regime compatibility.

Definition 4 (Regime compatibility) *A frozen growth equilibrium is compatible with an already active G regime iff*

$$\Xi\left(u_G^*\right) < \bar{\zeta}_+, \tag{48}$$

and a frozen fragility equilibrium is compatible with an already active F regime iff

$$\Xi\left(u_F^*\right) > \bar{\zeta}_-. \tag{49}$$

These are exactly the continuation conditions $u_G^* \in \mathcal{C}_G$ and $u_F^* \in \mathcal{C}_F$ from Equation (44). In the hysteresis band either regime can therefore be compatible, conditional on history.

Define the regime-specific exit margins

$$B_G(u) := \bar{\zeta}_+ - \Xi(u), \quad B_F(u) := \Xi(u) - \bar{\zeta}_-. \tag{50}$$

Hence compatibility is equivalent to $B_\sigma(u) > 0$. The forced-selection regions $\mathcal{D}_G$ and $\mathcal{D}_F$ are stricter objects: they identify states in which the current regime is selected independently of history.

Definition 5 (Dynamic local persistence) *A compatible state $u \in \mathcal{C}_G$ is locally persistence-improving under G if $L_{F_G}\Xi(u) < 0$ and persistence-eroding if $L_{F_G}\Xi(u) > 0$. A compatible state $u \in \mathcal{C}_F$ is locally persistence-improving under F if $L_{F_F}\Xi(u) > 0$ and persistence-eroding if $L_{F_F}\Xi(u) < 0$.*

The definition follows from

$$\dot{B}_G = -L_{F_G}\Xi, \quad \dot{B}_F = L_{F_F}\Xi. \tag{51}$$

Proposition 3 (Local invariance at the regime-exit boundaries) *Suppose the*

projected vector fields are locally Lipschitz. If

$$L_{F_G}\Xi(u) < 0 \quad \text{for every} \quad u \in \mathcal{S}_+, \tag{52}$$

then $\mathcal{C}_G$ *is locally positively invariant under the* G *flow at its exit boundary. If*

$$L_{F_F}\Xi(u) > 0 \quad \text{for every} \quad u \in \mathcal{S}_-, \tag{53}$$

then $\mathcal{C}_F$ *is locally positively invariant under the* F *flow at its exit boundary.*

Proof. For G, $\mathcal{C}_G = \{B_G > 0\}$ and on $\mathcal{S}_+$ we have $B_G = 0$. Equation (51) and Equation (52) imply $\dot{B}_G > 0$ on the boundary, so the vector field points strictly into $\mathcal{C}_G$. The standard tangency criterion gives local positive invariance. The proof for F is identical, using $B_F = 0$ on $\mathcal{S}_-$ and $\dot{B}_F = L_{F_F}\Xi > 0$.

The model therefore distinguishes four objects: conditional valuation, frozen-regime stationarity, history-consistent regime compatibility, and dynamic persistence under perturbations. The next section establishes that none of the earlier objects is, by itself, sufficient for the later one.

3. Equilibrium Viability and Regime Persistence

Section 2 developed a sustainable-finance framework in which valuation equilibria are embedded within an endogenous regime-switching system. The analysis identified the switching index Ξ, the hysteretic switching rule (43), and the compatibility conditions (48) and (49) that determine whether a given state remains consistent with the prevailing regime. The purpose of the present section is to characterize the implications of this switching geometry for equilibrium viability and regime persistence. In particular, we show that equilibrium existence does not in general imply regime persistence. Persistence depends on the position of the equilibrium relative to the transition frontier generated by the compatibility conditions. The results below characterize this frontier, establish conditions for equilibrium viability, and derive associated measures of transition risk. A numerical analysis is shown in **Tables A1-A10**.

3.1. Valuation Equilibrium versus Viability Equilibrium

Theorem 1 (Equilibrium-viability separation) *Let* $u_\sigma^* \in D^\circ$ *be a nondegenerate frozen-regime equilibrium,*

$$F_\sigma(u_\sigma^*) = 0, \quad \det J_\sigma(u_\sigma^*) \neq 0.$$

Then frozen-regime stationarity does not imply compatibility with the history-consistent hybrid regime. Specifically,

$$u_G^* \text{ is compatible with active } G \Leftrightarrow \Xi(u_G^*) < \bar{\zeta}_+,$$

whereas

$$u_F^* \text{ is compatible with active } F \Leftrightarrow \Xi(u_F^*) > \bar{\zeta}_-.$$

Moreover, compatibility alone does not imply dynamic persistence under perturbations: local invariance additionally requires the appropriate inward-

pointing condition in Proposition 3. Consequently,

valuation consistency $\not\Rightarrow$ regime compatibility $\not\Rightarrow$ dynamic persistence.

Proof. The equation $F_\sigma\left(u_\sigma^*\right)=0$ contains only the stationarity conditions of the frozen vector field. The active regime in the full model is instead determined by Equation (43). If G is active immediately before the state is evaluated, the rule retains G for all $\Xi<\bar{\zeta}_+$, including the continuation band, and switches to F when $\Xi\geq\bar{\zeta}_+$. Hence the growth compatibility condition is precisely $\Xi\left(u_G^*\right)<\bar{\zeta}_+$. Analogously, an active F regime persists for all $\Xi>\bar{\zeta}_-$ and switches to G when $\Xi\leq\bar{\zeta}_-$, yielding the fragility compatibility condition. Example 1 exhibits a nondegenerate root with $\Xi\left(u_G^*\right)>\bar{\zeta}_+$, proving by construction that stationarity does not imply compatibility. Finally, compatibility is only a membership condition. Under a perturbation near an exit boundary, the trajectory may move outward unless the corresponding Lie derivative has the inward sign stated in Proposition 3. Therefore, compatibility does not by itself establish dynamic persistence.

Corollary 1 (Greenium non-identification of resilience) *Fix a regime* σ *and factor normalization* $\gamma_{g,\sigma}$. *There exist states* $u,v\in D$ *with the same greenium but different compatibility and/or local-persistence classifications.*

Proof. By Equation (15), the hedged greenium is $\mu_{g,\sigma}=-\left(\bar{d}/a\right)\gamma_{g,\sigma}$. Hence two states with the same $\bar{d}$ have the same greenium. In contrast,

$$\Xi(u)=z+\vartheta(1-q)+\upsilon(1-\ell)-\rho_d\bar{d}-\rho_\lambda\lambda+\rho_c c$$

depends additionally on (λ,z,q,ℓ,c), and $L_{F_\sigma}\Xi$ depends on the full vector field. Holding $\bar{d}$ fixed, choose the remaining coordinates so that one state lies inside and another outside $\mathcal{C}_\sigma$, or so that both are compatible but the Lie derivative has opposite signs. The greenium is unchanged while the viability classification differs.

This result is a non-identification statement, not an empirical claim: a valuation statistic is many-to-one relative to the state information required for hybrid-regime persistence.

3.2. Equilibrium Compatibility and Endogenous Regime Failure

Theorem 2 (Compatibility and endogenous regime failure) *Let* u_σ^* *be a frozen-regime equilibrium. If*

$$\Xi\left(u_G^*\right)\geq\bar{\zeta}_+$$

for $\sigma=G$, or

$$\Xi\left(u_F^*\right)\leq\bar{\zeta}_-$$

for $\sigma=F$, then the full hybrid system cannot retain regime σ at u_σ^*. The regime change is generated endogenously by the state crossing its regime-specific exit boundary, even though the frozen vector field is stationary there.

Proof. At a frozen equilibrium, $F_\sigma\left(u_\sigma^*\right)=0$. But Equation (43) assigns F

whenever $\Xi \geq \bar{\zeta}_+$ and assigns G whenever $\Xi \leq \bar{\zeta}_-$. Thus a frozen G root at or above $\mathcal{S}_+$ is rejected by the switching map, and a frozen F root at or below $\mathcal{S}_-$ is rejected analogously. Stationarity of the frozen law and admissibility of that law in the hybrid system are therefore logically distinct.

3.3. The Transition-Resilience Frontier

Because hysteresis makes compatibility regime dependent, the relevant state space for viability is the augmented hybrid state space $D \times \{G, F\}$ rather than D alone. Define the regime-specific exit frontiers

$$\mathcal{F}_G := \mathcal{S}_+, \quad \mathcal{F}_F := \mathcal{S}_-, \quad \mathcal{F} := \mathcal{F}_G \cup \mathcal{F}_F. \tag{54}$$

The same physical state $u \in \mathcal{H}$ can therefore correspond to two different viable hybrid states (u, G) and (u, F), according to history.

Theorem 3 (Regime-specific transition-resilience frontier) *For an active growth regime, the signed distance coordinate*

$$B_G(u) = \bar{\zeta}_+ - \Xi(u) \tag{55}$$

is positive exactly on the continuation set $\mathcal{C}_G$, zero on $\mathcal{F}_G$, and negative beyond the growth exit boundary. For an active fragility regime,

$$B_F(u) = \Xi(u) - \bar{\zeta}_- \tag{56}$$

is positive exactly on $\mathcal{C}_F$, zero on $\mathcal{F}_F$, and negative beyond the fragility exit boundary. Since $\nabla \Xi \neq 0$, both frontier components are regular codimension-one hypersurfaces wherever they intersect the interior of D.

Proof. The sign claims follow directly from Equation (44). Moreover

$$\nabla \Xi = (-\rho_d, -\rho_\lambda, 1, -\vartheta, -\upsilon, \rho_c),$$

so $\partial \Xi / \partial z = 1$ and therefore $\nabla \Xi$ never vanishes. The regular level-set theorem implies that $\Xi^{-1}(\bar{\zeta}_+)$ and $\Xi^{-1}(\bar{\zeta}_-)$ are regular hypersurfaces in D°.

The theorem clarifies the role of the hysteresis band. It is not a region of incompatibility. Rather, it is a region in which both continuation margins are positive and regime identity must be carried as part of the state. Crossing $\mathcal{F}_G$ changes compatibility only for an active G regime; crossing $\mathcal{F}_F$ changes compatibility only for an active F regime.

3.4. Viability Equilibrium

The frontier result suggests a precise equilibrium notion on the augmented hybrid state space. A frozen state is not dynamically viable merely because it solves the stationarity equations; it must also be compatible with the active regime, and robustness to small perturbations requires an inward-pointing condition at the relevant exit boundary.

Definition 6 (Viability equilibrium) *An interior pair* (u_σ^*, σ) *is a regime-compatible viability equilibrium if*

$$F_\sigma(u_\sigma^*) = 0 \tag{57}$$

and

$$B_\sigma\left(u_\sigma^*\right) > 0. \tag{58}$$

It is locally robustly viable if, in addition, the relevant boundary satisfies the inward-pointing condition in Proposition 3.

Define the equilibrium resilience and fragility stocks

$$R_\sigma^* := \rho_d \bar{d}_\sigma^* + \rho_\lambda \lambda_\sigma^*, \quad H_\sigma^* := z_\sigma^* + \vartheta\left(1-q_\sigma^*\right) + \upsilon\left(1-\ell_\sigma^*\right) + \rho_c c_\sigma^*. \tag{59}$$

Then $\Xi\left(u_\sigma^*\right) = H_\sigma^* - R_\sigma^*$.

Theorem 4 (Equilibrium resilience balance) *Let* u_σ^* *be a frozen-regime equilibrium. Then*

$$\left(u_G^*, G\right) \text{ is compatible } \Leftrightarrow R_G^* - H_G^* > -\bar{\zeta}_+, \tag{60}$$

$$\left(u_F^*, F\right) \text{ is compatible } \Leftrightarrow H_F^* - R_F^* > \bar{\zeta}_-. \tag{61}$$

Equivalently,

$$B_G^* = \bar{\zeta}_+ + R_G^* - H_G^*, \tag{62}$$

$$B_F^* = H_F^* - R_F^* - \bar{\zeta}_-. \tag{63}$$

Thus valuation stationarity and viability impose independent restrictions.

Proof. By Equation (59), $\Xi\left(u_\sigma^*\right) = H_\sigma^* - R_\sigma^*$. For active G, Definition 4 requires $\Xi\left(u_G^*\right) < \bar{\zeta}_+$, which is equivalent to $R_G^* - H_G^* > -\bar{\zeta}_+$. For active F, compatibility requires $\Xi\left(u_F^*\right) > \bar{\zeta}_-$, equivalent to $H_F^* - R_F^* > \bar{\zeta}_-$. Substitution into Equation (50) gives Equations (62)-(63). None of these inequalities is contained in the vector equation $F_\sigma\left(u_\sigma^*\right) = 0$, as the explicit counterexample in Example 1 shows.

The signs of the margins retain a transparent economic interpretation. Since $B_G = \bar{\zeta}_+ - \Xi$, sustainable-growth compatibility increases with $\bar{d}, \lambda, q$, and ℓ and decreases with z and c. Conversely, $B_F = \Xi - \bar{\zeta}_-$ increases with z and c and decreases with $\bar{d}, \lambda, q$, and ℓ. These comparative statics concern distance to the regime-specific exit boundary; dynamic robustness additionally depends on $L_{F_\sigma}\Xi$.

4. Policy and Regulatory Implications

The results of Section 3 have important implications for sustainable-finance policy and regulation. Theorem 1 establishes that valuation equilibrium does not imply viability equilibrium. Corollary 1 shows that ESG pricing distortions are not sufficient indicators of system resilience. Theorem 2 demonstrates that regime incompatibility can generate endogenous regime failure even when a frozen equilibrium exists. Finally, Theorem 3 identifies a state-dependent frontier separating persistent from non-persistent sustainable-finance equilibria. These results imply that sustainable-finance policy cannot be based solely on valuation metrics. The relevant policy objective is not merely the pricing of sustainability, but the maintenance of regime compatibility and macro-financial resilience.

4.1. Why Valuation-Based ESG Metrics Are Insufficient

The preceding results characterize regime viability as a property of the switching geometry generated by the sustainability-fragility index (30). Viability depends on the position of the full state vector relative to the transition-resilience frontier and is therefore determined by the compatibility conditions (48) and (49).

This raises a natural identification problem. Financial markets do not directly observe the viability margins derived in Theorem 4. Instead, empirical and policy analysis typically relies on valuation-based indicators such as expected returns, ESG premia, and greenia. Theorem 5 shows that these valuation observables do not, in general, identify regime viability. States with identical expected returns and identical greenia may occupy different positions relative to the transition frontier and therefore possess different viability classifications. Consequently, regime resilience is a state-space property rather than a valuation statistic. Corollary 2 specializes this result to the greenium and shows that ESG pricing effects alone are insufficient to determine whether a sustainable growth regime remains viable.

Theorem 5 (Policy non-identification of regime viability)

Fix a regime $\sigma \in \{G, F\}$ and let

$$\mathcal{P}_\sigma : D \to \mathbb{R}^2$$

be the valuation-observable map

$$\mathcal{P}_\sigma(u) = \left(\mu_\sigma(u), \mu_{g,\sigma}(u)\right),$$

where μ_σ and $\mu_{g,\sigma}$ are determined by (11) and (15), respectively.

Suppose that the state space D contains valuation fibres along which the non-valuation state variables (λ, z, q, ℓ) can vary while $(\bar{d}, c)$ remain fixed, and that such variation can cross the relevant regime-specific exit boundary in (44). Then regime viability is not identified by valuation observables.

More precisely, there exist states $u, u' \in D$ such that

$$\mathcal{P}_\sigma(u) = \mathcal{P}_\sigma(u'),$$

but

$$\Xi(u) \neq \Xi(u').$$

Moreover, the two states may have different compatibility status:

$$u \in \mathcal{C}_\sigma, \quad u' \notin \mathcal{C}_\sigma.$$

Consequently, equilibrium expected returns and the greenium are not sufficient statistics for regime viability. A policy rule based only on valuation observables cannot, in general, determine whether the prevailing sustainable-finance regime remains compatible under the switching system (43).

Proof. Let

$$u = \left(\bar{d}, \lambda, z, q, \ell, c\right) \in D$$

and consider another state on the same valuation fibre,

$$u' = \left(\bar{d}, \lambda', z', q', \ell', c\right) \in D.$$

The two states agree in the valuation-relevant components $\bar{d}$ and c, but may differ in the state variables that enter the switching geometry. By (11),

$$\mu_\sigma(u) = \mu_{m,\sigma}\beta_{m,\sigma} - \frac{\bar{d}}{a}g + \pi_{c,\sigma}c\psi_\sigma.$$

Since u and u' have the same values of $\bar{d}$ and c,

$$\mu_\sigma(u') = \mu_{m,\sigma}\beta_{m,\sigma} - \frac{\bar{d}}{a}g + \pi_{c,\sigma}c\psi_\sigma = \mu_\sigma(u).$$

Similarly, by (15),

$$\mu_{g,\sigma}(u) = -\frac{\bar{d}}{a}\gamma_{g,\sigma},$$

and hence

$$\mu_{g,\sigma}(u') = -\frac{\bar{d}}{a}\gamma_{g,\sigma} = \mu_{g,\sigma}(u).$$

Therefore

$$\mathcal{P}_\sigma(u) = \mathcal{P}_\sigma(u').$$

However, by (30),

$$\Xi(u) = z + \vartheta(1-q) + \upsilon(1-\ell) - \rho_d\bar{d} - \rho_\lambda\lambda + \rho_c c,$$

whereas

$$\Xi(u') = z' + \vartheta(1-q') + \upsilon(1-\ell') - \rho_d\bar{d} - \rho_\lambda\lambda' + \rho_c c.$$

Subtracting,

$$\Xi(u') - \Xi(u) = (z'-z) - \vartheta(q'-q) - \upsilon(\ell'-\ell) - \rho_\lambda(\lambda'-\lambda).$$

The right-hand side depends on systemic stress, information quality, market liquidity, and participation, none of which is identified by (11) or (15) once $(\bar{d}, c)$ are fixed. Hence

$$\mathcal{P}_\sigma(u) = \mathcal{P}_\sigma(u') \not\Rightarrow \Xi(u) = \Xi(u').$$

For the sustainable-growth regime, (44) gives

$$u \in \mathcal{C}_G \iff \Xi(u) < \bar{\zeta}_+.$$

By the threshold-crossing assumption, there exist states on the same valuation fibre such that

$$\Xi(u) < \bar{\zeta}_+ < \Xi(u'),$$

while

$$\mathcal{P}_G(u) = \mathcal{P}_G(u').$$

Thus

$$u \in \mathcal{C}_G, \quad u' \notin \mathcal{C}_G.$$

For the financial-fragility regime, (44) gives

$$u \in \mathcal{C}_F \iff \Xi(u) > \bar{\zeta}_-.$$

Again, by the threshold-crossing assumption, there exist states on the same valuation fibre such that

$$\Xi(u) > \bar{\zeta}_- > \Xi(u'),$$

while

$$\mathcal{P}_F(u) = \mathcal{P}_F(u').$$

Thus

$$u \in \mathcal{C}_F, \quad u' \notin \mathcal{C}_F.$$

Finally, by (43), regime compatibility is determined by the value of $\Xi(u)$ relative to the thresholds $\bar{\zeta}_-$ and $\bar{\zeta}_+$. Since there exist states $u, u' \in D$ such that

$$\mathcal{P}_\sigma(u) = \mathcal{P}_\sigma(u'),$$

but

$$\Xi(u) \neq \Xi(u'),$$

the value of Ξ is not identified by $\mathcal{P}_\sigma$. Moreover, there exist states satisfying

$$\mathcal{P}_\sigma(u) = \mathcal{P}_\sigma(u'),$$

for which

$$u \in \mathcal{C}_\sigma, \quad u' \notin \mathcal{C}_\sigma.$$

Hence

$$\mathcal{P}_\sigma(u) = \mathcal{P}_\sigma(u') \not\Rightarrow (u \in \mathcal{C}_\sigma \Leftrightarrow u' \in \mathcal{C}_\sigma).$$

Therefore, the viability classification induced by (44), (44), and (43) is not identifiable from the valuation-observable map $\mathcal{P}_\sigma$.

Corollary 2 (Greenium non-identification of sustainable-growth viability)

The greenium does not identify sustainable-growth viability.

More precisely, there exist states $u, u' \in D$ such that

$$\mu_{g,G}(u) = \mu_{g,G}(u'),$$

but

$$u \in \mathcal{C}_G, \quad u' \notin \mathcal{C}_G.$$

Equivalently,

$$\mu_{g,G}(u) = \mu_{g,G}(u') \not\Rightarrow (u \in \mathcal{C}_G \Leftrightarrow u' \in \mathcal{C}_G).$$

Therefore, the greenium is not a sufficient statistic for sustainable-growth viability.

Proof. By (15),

$$\mu_{g,G} = -\frac{\bar{d}}{a}\gamma_{g,G}.$$

Hence the greenium depends only on the sustainability-demand component $\bar{d}$. In contrast, sustainable-growth viability is determined by the sustainability-

fragility index (30),

$$\Xi = z + \vartheta(1-q) + \upsilon(1-\ell) - \rho_d \bar{d} - \rho_\lambda \lambda + \rho_c c,$$

which depends on the full state vector

$$u = (\bar{d}, \lambda, z, q, \ell, c).$$

By (44),

$$u \in \mathcal{C}_G \iff \Xi(u) < \bar{\zeta}_+.$$

Theorem 5 establishes that there exist states

$$u = (\bar{d}, \lambda, z, q, \ell, c), \quad u' = (\bar{d}, \lambda', z', q', \ell', c),$$

with identical valuation observables and therefore identical greenia,

$$\mu_{g,G}(u) = \mu_{g,G}(u'),$$

while

$$\Xi(u) \neq \Xi(u').$$

Moreover, there exist such states satisfying

$$\Xi(u) < \bar{\zeta}_+ < \Xi(u').$$

Using (44), it follows that

$$u \in \mathcal{C}_G, \quad u' \notin \mathcal{C}_G.$$

Hence two states may generate the same greenium while possessing different viability classifications. Therefore

$$\mu_{g,G}(u) = \mu_{g,G}(u') \not\Rightarrow (u \in \mathcal{C}_G \iff u' \in \mathcal{C}_G),$$

and the greenium does not identify sustainable-growth viability.

4.2. Compatibility-Based Regulation

The preceding results characterize regime viability as a property of the compatibility margins generated by the switching geometry. Theorem 4 shows that viability depends on the balance between resilience and fragility forces, while Theorem 5 establishes that this balance cannot, in general, be inferred from valuation observables alone.

The policy question is therefore not how to preserve a particular equilibrium price configuration, but how to maintain the compatibility conditions required for regime persistence. In the present framework, policy operates by altering the primitives that determine the sustainability-fragility index and hence the position of the economy relative to the transition-resilience frontier.

To study these effects, we introduce the sustainable-growth compatibility margin (64), which measures the distance of the current state from the sustainable-growth viability boundary. Theorem 6 then characterizes how policy-induced changes in systemic stress, information quality, market liquidity, sustainable-investment demand, investor participation, and climate pressure affect this margin and thereby

alter the size of the sustainable-growth viability region.

The resulting characterization identifies the fundamental policy channels through which sustainable-finance regulation can increase regime resilience and reduce the likelihood of endogenous regime failure. To formalize this idea, define the sustainable-growth compatibility margin

$$M_G(u) = \bar{\zeta}_+ - \Xi(u). \tag{64}$$

The quantity $M_G(u)$ measures the distance between the prevailing state and the sustainable-growth compatibility boundary (48). The sustainable-growth regime is compatible if and only if

$$M_G(u) \geq 0.$$

Moreover,

$$M_G(u) = 0$$

coincides with the viability frontier separating sustainable-growth persistence from regime failure.

Theorem 6 (Primitive policy dominance and viability-region expansion)

Let Π_1 and Π_2 be two policy configurations, and suppose that

$$\vartheta, \upsilon, \rho_d, \rho_\lambda, \rho_c > 0.$$

Assume that, for every $u \in D$, policy Π_1 weakly dominates policy Π_2 in the following primitive sense:

$$z_{\Pi_1}(u) \leq z_{\Pi_2}(u), \tag{65}$$

$$q_{\Pi_1}(u) \geq q_{\Pi_2}(u), \tag{66}$$

$$\ell_{\Pi_1}(u) \geq \ell_{\Pi_2}(u), \tag{67}$$

$$\bar{d}_{\Pi_1}(u) \geq \bar{d}_{\Pi_2}(u), \tag{68}$$

$$\lambda_{\Pi_1}(u) \geq \lambda_{\Pi_2}(u), \tag{69}$$

$$c_{\Pi_1}(u) \leq c_{\Pi_2}(u). \tag{70}$$

Then

$$\Xi_{\Pi_1}(u) \leq \Xi_{\Pi_2}(u) \quad \forall u \in D. \tag{71}$$

Consequently,

$$M_G^{\Pi_1}(u) \geq M_G^{\Pi_2}(u) \quad \forall u \in D, \tag{72}$$

and the sustainable-growth viability regions satisfy

$$\mathcal{C}_G(\Pi_2) \subseteq \mathcal{C}_G(\Pi_1). \tag{73}$$

If at least one of (65)-(70) is strict at a state u, then

$$\Xi_{\Pi_1}(u) < \Xi_{\Pi_2}(u), \quad M_G^{\Pi_1}(u) > M_G^{\Pi_2}(u). \tag{74}$$

Thus primitive policy improvements that weakly reduce systemic stress and climate-pressure exposure, weakly improve information quality and market liquidity,

and weakly increase sustainable-investment demand and participation weakly expand the sustainable-growth viability region.

Proof. By (30), the policy-modified sustainability-fragility index is

$$\Xi_{\Pi}(u) = z_{\Pi}(u) + \vartheta\left(1 - q_{\Pi}(u)\right) + \upsilon\left(1 - \ell_{\Pi}(u)\right) - \rho_d \bar{d}_{\Pi}(u) - \rho_{\lambda}\lambda_{\Pi}(u) + \rho_c c_{\Pi}(u).$$

Therefore

$$\begin{aligned}\Xi_{\Pi_1}(u) - \Xi_{\Pi_2}(u) = &\left(z_{\Pi_1}(u) - z_{\Pi_2}(u)\right) - \vartheta\left(q_{\Pi_1}(u) - q_{\Pi_2}(u)\right)\\ &- \upsilon\left(\ell_{\Pi_1}(u) - \ell_{\Pi_2}(u)\right) - \rho_d\left(\bar{d}_{\Pi_1}(u) - \bar{d}_{\Pi_2}(u)\right)\\ &- \rho_{\lambda}\left(\lambda_{\Pi_1}(u) - \lambda_{\Pi_2}(u)\right) + \rho_c\left(c_{\Pi_1}(u) - c_{\Pi_2}(u)\right).\end{aligned}$$

Since

$$\vartheta, \upsilon, \rho_d, \rho_{\lambda}, \rho_c > 0,$$

conditions (65)-(70) imply that every term on the right-hand side is weakly non-positive. Hence

$$\Xi_{\Pi_1}(u) - \Xi_{\Pi_2}(u) \le 0,$$

which proves (71). By (64),

$$M_G^{\Pi}(u) = \bar{\zeta}_+ - \Xi_{\Pi}(u).$$

Using (71),

$$M_G^{\Pi_1}(u) = \bar{\zeta}_+ - \Xi_{\Pi_1}(u) \ge \bar{\zeta}_+ - \Xi_{\Pi_2}(u) = M_G^{\Pi_2}(u),$$

which proves (72). By (44),

$$\mathcal{C}_G(\Pi) = \left\{u \in D : \Xi_{\Pi}(u) \le \bar{\zeta}_-\right\}.$$

Let

$$u \in \mathcal{C}_G(\Pi_2).$$

Then

$$\Xi_{\Pi_2}(u) < \bar{\zeta}_+.$$

Together with (71), this gives

$$\Xi_{\Pi_1}(u) \le \Xi_{\Pi_2}(u) \le \bar{\zeta}_-.$$

Therefore

$$u \in \mathcal{C}_G(\Pi_1).$$

Since this holds for every $u \in \mathcal{C}_G(\Pi_2)$,

$$\mathcal{C}_G(\Pi_2) \subseteq \mathcal{C}_G(\Pi_1),$$

which proves (73). Finally, if at least one of (65)-(70) is strict at u, then the corresponding term in

$$\Xi_{\Pi_1}(u) - \Xi_{\Pi_2}(u)$$

is strictly negative, while all remaining terms are weakly non-positive. Hence

$$\Xi_{\Pi_1}(u) < \Xi_{\Pi_2}(u).$$

Using (64), this implies

$$M_G^{\Pi_1}(u) > M_G^{\Pi_2}(u).$$

This proves (74).

Corollary 3 (Independent policy channels for viability expansion)
Suppose that

$$\vartheta, \upsilon, \rho_d, \rho_\lambda, \rho_c > 0.$$

Then the sustainability-fragility index (30) satisfies

$$\frac{\partial \Xi}{\partial z} > 0, \quad \frac{\partial \Xi}{\partial q} < 0, \quad \frac{\partial \Xi}{\partial \ell} < 0, \quad \frac{\partial \Xi}{\partial \bar{d}} < 0, \quad \frac{\partial \Xi}{\partial \lambda} < 0, \quad \frac{\partial \Xi}{\partial c} > 0.$$

Hence each of the following primitive policy changes weakly increases the sustainable-growth compatibility margin and weakly expands the sustainable-growth viability region, provided the remaining fragility-relevant primitives are held fixed or weakly improved:

$$z \downarrow, \quad q \uparrow, \quad \ell \uparrow, \quad \bar{d} \uparrow, \quad \lambda \uparrow, \quad c \downarrow.$$

Therefore, sustainable-growth viability is not governed by a single policy instrument but by six structurally distinct channels acting through the sustainability-fragility index: systemic-stress reduction, information-quality improvement, liquidity enhancement, sustainable demand support, investor-participation strengthening, and climate-pressure reduction.

Proof. By (30),

$$\Xi = z + \vartheta(1-q) + \upsilon(1-\ell) - \rho_d \bar{d} - \rho_\lambda \lambda + \rho_c c.$$

Therefore

$$\frac{\partial \Xi}{\partial z} = 1, \quad \frac{\partial \Xi}{\partial q} = -\vartheta, \quad \frac{\partial \Xi}{\partial \ell} = -\upsilon, \quad \frac{\partial \Xi}{\partial \bar{d}} = -\rho_d, \quad \frac{\partial \Xi}{\partial \lambda} = -\rho_\lambda, \quad \frac{\partial \Xi}{\partial c} = \rho_c.$$

Since

$$\vartheta, \upsilon, \rho_d, \rho_\lambda, \rho_c > 0,$$

the stated signs follow. By (64),

$$M_G(u) = \bar{\zeta}_+ - \Xi(u).$$

Hence any primitive change that weakly lowers Ξ weakly raises M_G. The derivative signs imply that each of

$$z \downarrow, \quad q \uparrow, \quad \ell \uparrow, \quad \bar{d} \uparrow, \quad \lambda \uparrow, \quad c \downarrow$$

weakly lowers Ξ, provided the remaining fragility-relevant primitives are held fixed or weakly improved. Therefore each channel weakly increases the sustainable-growth compatibility margin. Finally, by Theorem 6, any policy-induced weak increase in the compatibility margin generated by primitive dominance weakly

expands the sustainable-growth viability region. Hence each channel constitutes an independent policy lever for viability expansion.

4.3. Transition-Risk Monitoring

The preceding results characterize equilibrium viability as a static property of the switching geometry. Theorems 3, 4, and 6 identify the conditions under which a sustainable-growth equilibrium remains compatible with the regime supporting it and how policy can alter the size of the viability region. However, regime persistence is ultimately a dynamic concept. The current viability status of an equilibrium does not by itself reveal whether the economy is moving toward greater resilience or toward the transition frontier. Two economies may be equally distant from the frontier while facing very different transition prospects because their underlying state dynamics differ. The relevant object is therefore not only the compatibility margin itself, but also its endogenous evolution under the sustainable-growth vector field. Transition risk emerges when the compatibility margin contracts and the economy moves toward the frontier separating regime persistence from regime failure. To characterize this mechanism, we study the dynamics of the sustainable-growth compatibility margin and derive a local measure of transition-risk intensity. Theorem 7 shows that transition risk is jointly determined by the current distance from the frontier and the rate at which the endogenous dynamics erode that distance. Corollary 4 then provides an operational early-warning indicator based on these two quantities.

The resulting measure links the static geometry of equilibrium viability to the dynamic probability of regime transition and provides a quantitative framework for monitoring the resilience of sustainable-finance equilibria. To characterize this effect, define the sustainable-growth compatibility margin

$$M_G(u) = \bar{\zeta}_+ - \Xi(u), \tag{75}$$

and its evolution along trajectories of (20),

$$\dot{M}_G(u) = -L_{F_G}\Xi(u). \tag{76}$$

The quantity (76) measures the instantaneous rate at which the economy approaches or moves away from the transition frontier.

Theorem 7 (Local transition-time ordering)

Let $u \in \mathcal{C}_G$ satisfy

$$M_G(u) > 0, \quad L_{F_G}\Xi(u) > 0.$$

Let $\phi_G(t,u)$ denote the local flow generated by the sustainable-growth vector field F_G, and define the local transition time by

$$\tau_G(u) := \inf\left\{t \geq 0 : M_G\left(\phi_G(t,u)\right) = 0\right\}.$$

Then, to first order around u,

$$\tau_G(u) = \frac{M_G(u)}{L_{F_G}\Xi(u)} + o(1).$$

Equivalently, the local transition-risk intensity is

$$\mathcal{R}_G^{\mathrm{loc}}(u) := \frac{1}{\tau_G^{\mathrm{loc}}(u)} = \frac{L_{F_G}\Xi(u)}{M_G(u)}.$$

Consequently, local transition risk is increasing in $L_{F_G}\Xi(u)$ and decreasing in $M_G(u)$.

Proof. By (75),

$$M_G(u) = \overline{\zeta}_+ - \Xi(u).$$

Along the sustainable-growth flow

$$t \mapsto \phi_G(t,u),$$

the margin evolves according to

$$\frac{\mathrm{d}}{\mathrm{d}t} M_G\left(\phi_G(t,u)\right) = L_{F_G} M_G\left(\phi_G(t,u)\right).$$

Since

$$M_G = \overline{\zeta}_+ - \Xi,$$

we obtain

$$L_{F_G} M_G(u) = -L_{F_G}\Xi(u).$$

Using (34) and (35),

$$L_{F_G}\Xi(u) = \nabla\Xi(u)^{\top} F_G(u),$$

that is,

$$\begin{aligned} L_{F_G}\Xi(u) = &-\rho_d F_G^d(u) - \rho_\lambda F_G^\lambda(u) + F_G^z(u) \\ &- \vartheta F_G^q(u) - \upsilon F_G^\ell(u) + \rho_c F_G^c(u). \end{aligned} \tag{77}$$

Hence

$$\dot{M}_G(u) = -\left[-\rho_d F_G^d(u) - \rho_\lambda F_G^\lambda(u) + F_G^z(u) - \vartheta F_G^q(u) - \upsilon F_G^\ell(u) + \rho_c F_G^c(u)\right].$$

A first-order Taylor expansion of the margin along the flow gives

$$M_G\left(\phi_G(t,u)\right) = M_G(u) + tL_{F_G} M_G(u) + o(t).$$

Substituting

$$L_{F_G} M_G(u) = -L_{F_G}\Xi(u)$$

yields

$$M_G\left(\phi_G(t,u)\right) = M_G(u) - tL_{F_G}\Xi(u) + o(t).$$

The local transition time is the time at which the linearized margin reaches zero. Thus

$$0 = M_G(u) - tL_{F_G}\Xi(u).$$

Since

$$L_{F_G}\Xi(u) > 0,$$

this equation has the positive solution

$$t = \frac{M_G(u)}{L_{F_G}\Xi(u)}.$$

Therefore

$$\tau_G^{\mathrm{loc}}(u) = \frac{M_G(u)}{L_{F_G}\Xi(u)}.$$

Taking the reciprocal gives the local transition-risk intensity

$$\mathcal{R}_G^{\mathrm{loc}}(u) = \frac{1}{\tau_G^{\mathrm{loc}}(u)} = \frac{L_{F_G}\Xi(u)}{M_G(u)}.$$

Hence

$$\frac{\partial \mathcal{R}_G^{\mathrm{loc}}}{\partial L_{F_G}\Xi} = \frac{1}{M_G(u)} > 0,$$

and

$$\frac{\partial \mathcal{R}_G^{\mathrm{loc}}}{\partial M_G} = -\frac{L_{F_G}\Xi(u)}{M_G(u)^2} < 0.$$

Thus local transition risk increases with switching pressure and decreases with compatibility-margin distance from the frontier.

Corollary 4 (Early-warning indicator)

Define the local early-warning indicator by

$$\mathcal{R}_G^{\mathrm{loc}}(u) = \frac{L_{F_G}\Xi(u)}{M_G(u)}.$$

For all $u \in \mathcal{C}_G$ such that

$$M_G(u) > 0, \quad L_{F_G}\Xi(u) > 0,$$

the indicator satisfies

$$\frac{\partial \mathcal{R}_G^{\mathrm{loc}}}{\partial L_{F_G}\Xi} > 0, \quad \frac{\partial \mathcal{R}_G^{\mathrm{loc}}}{\partial M_G} < 0.$$

In particular,

$$M_G(u) \downarrow 0, \quad L_{F_G}\Xi(u) > 0,$$

implies

$$\mathcal{R}_G^{\mathrm{loc}}(u) \to +\infty.$$

Hence states close to the sustainable-growth transition frontier and moving toward higher fragility are locally vulnerable to regime failure.

Proof. The first two inequalities follow directly from Theorem 7. Indeed,

$$\mathcal{R}_G^{\mathrm{loc}}(u) = \frac{L_{F_G}\Xi(u)}{M_G(u)}.$$

Therefore

$$\frac{\partial \mathcal{R}_G^{\mathrm{loc}}}{\partial L_{F_G}\Xi} = \frac{1}{M_G(u)} > 0$$

and

$$\frac{\partial \mathcal{R}_G^{\mathrm{loc}}}{\partial M_G} = -\frac{L_{F_G}\Xi(u)}{M_G(u)^2} < 0.$$

If

$$M_G(u) \downarrow 0$$

while

$$L_{F_G}\Xi(u) > 0$$

remains positive, then

$$\frac{L_{F_G}\Xi(u)}{M_G(u)} \to +\infty.$$

Thus the state is simultaneously close to the transition frontier and moving toward it, so local transition-risk intensity diverges.

5. Discussion

The paper establishes that sustainable-finance equilibria must be evaluated along two distinct dimensions; valuation and viability (**Tables A1-A10**). The distinction begins with Proposition 2, which shows that a frozen-regime equilibrium can be locally well defined, and Example 1, which shows constructively that local equilibrium existence does not imply regime compatibility. This is the central conceptual separation of the model. Standard sustainable-finance theory studies how preferences, beliefs, climate exposures, and nonpecuniary motives enter prices, expected returns, portfolio allocations, and financing costs [1] [2] [4] [5] [7]. The present framework shows that these valuation conditions are incomplete when the regime supporting the equilibrium is selected by an endogenous switching rule. Theorem 1 formalizes this incompleteness. A state may satisfy the frozen-equilibrium condition (45) and still fail the compatibility inequalities (48)-(49). Theorem 2 then gives the economic content of this failure: regime breakdown need not be caused by an external shock, a collapse of pricing, or nonexistence of equilibrium. It can arise because the equilibrium itself lies outside the admissible domain generated by the switching geometry. Thus the paper moves sustainable finance from a theory of equilibrium pricing to a theory of admissible equilibrium persistence. This perspective changes the interpretation of ESG premia. Empirical work documents sustainability premia, green bond pricing effects, ESG fund flows, and investor-demand channels [28] [29] [31] [34]-[37]. Those effects are real valuation effects, but Corollary 1, Theorem 5, and Corollary 2 show that they do not identify resilience. The reason is that the greenium and expected-return observables depend on valuation-relevant components of the state,

whereas viability depends on the full macro-financial vector $u=(\bar{d},\lambda,z,q,\ell,c)$ through (30). Hence two economies can display the same greenium while differing in participation, systemic stress, disclosure quality, liquidity, or climate-pressure exposure. A pricing statistic is therefore not a sufficient statistic for sustainable-growth viability. Theorem 3 provides the geometric object behind this non-identification. The transition-resilience frontier is not an asset-pricing boundary; it is a codimension-one switching boundary separating admissible from inadmissible regimes. Theorem 4 gives this geometry economic content by decomposing viability into a balance between the resilience stock R_σ^* and the fragility stock H_σ^*. This connects the model to empirical evidence that sustainable-finance outcomes depend not only on demand, but also on disclosure, engagement, ownership, liquidity, and financial frictions [9] [15] [16] [38] [39] [41]. In the model, these variables matter because they shift the economy relative to the viability frontier. The policy implication is correspondingly sharp. Theorem 6 shows that policy improves sustainable-growth viability when it lowers systemic stress and climate-pressure exposure while raising information quality, liquidity, sustainable-investment demand, and participation. Corollary 3 shows that these are independent policy channels. This matters because sustainable-finance policy is often evaluated through price effects: whether it lowers green financing costs, increases ESG demand, or raises sustainability premia. The model implies that such criteria are insufficient. A policy can affect prices without expanding the viability region, and a successful policy is one that improves the compatibility margin M_G, not merely one that changes equilibrium returns. The dynamic results further strengthen this point. Climate-finance models often interpret transition risk through carbon repricing, stranded assets, policy shocks, or changing climate expectations [8] [10]-[13] [40]. Theorem 7 instead characterizes transition risk as a local state-space quantity. The relevant object is not only the distance $M_G(u)$ from the frontier, but also the drift $L_{F_G}\Xi(u)$ toward it. Corollary 4 translates this into the early-warning indicator $\mathcal{R}_G^{\mathrm{loc}}(u)=L_{F_G}\Xi(u)/M_G(u)$, which diverges as the compatibility margin collapses while switching pressure remains positive. Transition risk is therefore a property of endogenous motion near the frontier, not only a response to exogenous climate news. The broader theoretical contribution is to embed sustainable finance in a state-constrained equilibrium framework. Classical asset-pricing and sustainable-finance models ask whether sustainability is priced. This paper asks whether the regime supporting those prices can persist. The difference is captured by replacing the valuation problem $F_\sigma(u)=0$ with the viability problem $F_\sigma(u)=0$ together with $u\in\mathcal{C}_\sigma$, conditional on the active regime history. This stronger requirement connects sustainable finance to macro-financial fragility models in which endogenous state variables determine systemic vulnerability [17] [18] [20]. The novelty is that fragility is not only financial: it is generated by the interaction of ESG demand, participation, stress, information quality, liquidity, and climate concern. Jointly, Proposition 2, Example 1, Theorem 1, Corollary 1, Theorem 2, Theorem 3, Theorem

4, Theorem 5, Corollary 2, Theorem 6, Corollary 3, Theorem 7, and Corollary 4 establish a single conclusion. Sustainable finance is not only about how sustainability is capitalized into prices. It is about whether the macro-financial state generated by those prices remains compatible with the regime required for sustainable growth.

A central advantage of the viability-equilibrium framework is that each theoretical state variable admits a natural empirical counterpart. Table 1 summarizes the mapping between the model's latent viability state and observable variables widely studied in the sustainable-finance, climate-finance, asset-pricing, and financial-stability literatures.

Table 1. Empirical interpretation of the theoretical state variables.

Model object	Economic interpretation	Observable counterpart
Sustainable-investment demand	Investor demand for sustainable assets	ESG fund flows; green fund AUM; ESG ETF inflows
Investor participation	Breadth of participation in sustainable markets	Number/share of ESG investors; fund ownership concentration
Information quality	Reliability of sustainability information	ESG rating dispersion; disclosure scores; greenwashing controversy indicators
Market liquidity	Ability to rebalance without destabilising prices	Bid-ask spreads; turnover; Amihud illiquidity; market depth
Systemic stress	Fragility of financial conditions	VIX; financial stress indices; credit spreads
Climate concern	Intensity of climate-risk salience	Climate-policy uncertainty; news-based climate concern indices
Viability frontier	Boundary of regime persistence	Threshold level of the fragility index Ξ_t

Sustainable-investment demand can be measured through ESG fund flows, sustainable-fund assets under management, and ESG ETF inflows [5] [7] [35]. Investor participation corresponds to the breadth and concentration of ownership in sustainable assets, which can be measured through institutional ownership, ownership breadth, and concentration indices [42]. Information quality can be proxied through ESG-rating disagreement, sustainability disclosure quality, and greenwashing indicators [39] [43]. Market liquidity corresponds to observable measures such as bid-ask spreads, turnover ratios, market depth, and Amihud illiquidity [15] [16]. Systemic stress can be measured using the VIX, financial-stress indices, credit spreads, and systemic-risk measures such as CoVaR [19] [21]. Climate concern corresponds to the salience of climate-related risks and can be proxied through climate-policy uncertainty, climate-news measures, and climate-risk indicators [8] [14] [44]. Finally, the viability frontier corresponds to an empirically estimated boundary separating persistent from non-persistent sustainable-finance regimes and may be identified using threshold and regime-switching methods [45] [46].

The framework generates several empirically testable implications that help

organize a rapidly expanding and sometimes fragmented literature on sustainable finance.

First, valuation outcomes and systemic resilience need not move together. A large empirical literature documents sustainability premia, greeniums, and persistent investor demand for sustainable assets [5] [7]. Existing studies generally interpret these outcomes as evidence that sustainability characteristics are being priced by financial markets. **Table 1** shows, however, that the viability state depends not only on sustainable-investment demand but also on investor participation, information quality, market liquidity, systemic stress, and climate concern. Consequently, positive sustainability premia may coexist with deteriorating liquidity conditions, increasing ESG-rating dispersion, rising ownership concentration, elevated systemic risk, or declining information quality. The model therefore implies that sustainability premia and greeniums are not sufficient statistics for the resilience of a sustainable-finance regime.

Second, economies exhibiting similar ESG premia may nevertheless face substantially different transition risks. A growing climate-finance literature emphasizes that financial vulnerability depends not only on asset valuations but also on network structure, systemic interconnectedness, information quality, and financial-system fragility [14] [21] [47]. The viability framework provides a formal theoretical structure for this observation. Two economies may exhibit similar asset prices, expected returns, sustainability premia, or greeniums while differing substantially in ownership concentration, market liquidity, ESG-rating disagreement, climate-policy uncertainty, or systemic stress. Such economies occupy different locations within the viability state space and therefore possess different probabilities of regime persistence. The framework thus distinguishes valuation similarity from viability similarity.

Third, the model predicts that major sustainable-finance disruptions should be preceded by deterioration in viability indicators rather than necessarily by a collapse in sustainable-investment demand. Empirical studies of financial crises and systemic instability frequently identify declining liquidity, rising uncertainty, increasing fragility, and worsening informational conditions as leading indicators of financial stress [15] [16] [19] [21]. Within the present framework, these variables provide information about distance to the viability frontier. In terms of the observable quantities listed in **Table 1**, transition events should be preceded by widening bid-ask spreads, rising Amihud illiquidity, increasing ESG-rating disagreement, greater ownership concentration, elevated financial-stress measures, widening credit spreads, and increasing climate-policy uncertainty. Importantly, the model predicts that these developments may occur while sustainable-investment demand remains positive and sustainability premia remain observable.

Fourth, the framework predicts that information quality constitutes a separate dimension of sustainable-finance stability. Recent evidence demonstrates substantial disagreement among ESG rating providers and high levels of measurement divergence [39]. The viability framework implies that such disagreement is not

merely a measurement problem but may affect the persistence of sustainable-finance equilibria by weakening the informational foundations upon which sustainable-investment demand is based. Consequently, increasing ESG-rating dispersion should be associated with greater fragility even when aggregate sustainable investment remains unchanged.

Fifth, the model predicts that investor participation and ownership structure affect regime resilience independently of aggregate sustainable-investment demand. Concentrated ownership structures can leave sustainable-finance markets vulnerable to coordinated withdrawals or common shocks, whereas broader participation increases the robustness of the regime. This implication links the viability framework to the literature on ownership breadth and market stability [42] and suggests that ownership concentration should possess incremental explanatory power for sustainable-finance stability beyond that contained in valuation measures alone.

More generally, **Table 1** provides a theoretical identification structure linking sustainable-finance valuations to the broader conditions governing regime persistence. The framework therefore clarifies which empirical variables are required to distinguish valuation equilibrium from viability equilibrium. Valuation equilibrium may be identified through prices, expected returns, greeniums, and sustainable-investment flows. Viability equilibrium, by contrast, additionally requires information on participation breadth, ownership concentration, information quality, market liquidity, systemic stress, climate-risk salience, and the economy's position relative to the empirically estimated viability frontier.

The contribution is therefore not the introduction of a new empirical indicator but the identification of a distinct equilibrium object. The sustainable-finance literature has primarily focused on whether sustainability characteristics are priced in financial markets [5] [7]. The present framework complements this literature by identifying the conditions under which the regime supporting those pricing outcomes remains viable. Empirically, this implies that sustainable-finance resilience cannot be inferred from valuation measures alone but requires joint analysis of the state variables summarized in **Table 1**.

From Viability Theory to Empirical Implementation

The analytical framework identifies objects that can in principle be taken to data, but the computations in this paper are not an empirical validation of the model. The state paths, transition labels, and switching frontier in Appendix 6 are generated from the same specified dynamics and thresholds that define the theory. They therefore serve only as numerical illustrations of internal operation, non-identification, and hysteretic persistence.

An empirical application would require independent measurements or estimates of $\bar{d}, \lambda, z, q, \ell$, and c, together with an independently estimated switching rule. Valuation relations could be confronted with observed returns and greeniums, while regime-persistence claims would require external transition outcomes or duration data. In particular, predictive performance computed from

model-generated transition labels cannot establish out-of-sample forecasting power for real financial regimes. The numerical appendix is therefore framed strictly as a reproducible computational illustration and as a bridge to future empirical work.

6. Conclusions

This paper develops a viability-based framework for sustainable finance under endogenous regime switching. The analysis demonstrates that valuation and persistence constitute distinct dimensions of equilibrium. While existing sustainable finance models focus primarily on how sustainability characteristics are incorporated into prices, the framework developed here focuses on whether the macro-financial conditions supporting those prices remain capable of persisting over time.

The principal contribution of the paper is the introduction of viability equilibrium as a separate equilibrium object. The theoretical results establish that sustainability premia, greeniums, and related valuation observables do not generally identify resilience. The numerical illustrations reproduce this distinction within the model-generated environment: states with similar valuation outcomes can possess markedly different viability classifications and transition risks, while state-based measures recover the imposed transition mechanism more accurately than valuation-only measures.

More broadly, the paper suggests that equilibrium analysis under endogenous regime switching cannot be reduced to a problem of valuation alone. Whenever economic systems are governed by thresholds, feedback effects, and state-dependent transitions, persistence becomes an economic object in its own right. The viability frontier therefore provides a framework for analysing not only how equilibrium outcomes are determined, but also whether the conditions supporting those outcomes remain admissible under the system's own dynamics.

The principal limitation of the present analysis is also one of its strengths. The framework is developed at a level of abstraction that isolates the geometric relationship between valuation, viability, and regime persistence without imposing institution-specific assumptions or market-specific calibration choices. This abstraction permits the identification of mechanisms that are potentially common across a wide class of sustainable-finance environments, but it does not by itself establish how the viability frontier should be measured in any particular market.

The next stage of the research programme is therefore empirical rather than conceptual. An important challenge is the construction of observable proxies for the state variables entering the viability framework and the estimation of transition frontiers using financial, sustainability, and macroeconomic data. Such an extension would allow the viability-equilibrium concept developed here to be translated from a theoretical characterization of regime persistence into an empirically measurable object suitable for forecasting transition risk and evaluating policy interventions.

Conflicts of Interest

The author declares no conflicts of interest regarding the publication of this paper.

References

[1] Heinkel, R., Kraus, A. and Zechner, J. (2001) The Effect of Green Investment on Corporate Behavior. *The Journal of Financial and Quantitative Analysis*, **36**, 431-449. https://doi.org/10.2307/2676219

[2] Fama, E.F. and French, K.R. (2007) Disagreement, Tastes, and Asset Prices. *Journal of Financial Economics*, **83**, 667-689. https://doi.org/10.1016/j.jfineco.2006.01.003

[3] Friedman, H.L. and Heinle, M.S. (2016) Taste, Information, and Asset Prices: Implications for the Valuation of CSR. *Review of Accounting Studies*, **21**, 740-767. https://doi.org/10.1007/s11142-016-9359-x

[4] Hart, O. and Zingales, L. (2017) Companies Should Maximize Shareholder Welfare Not Market Value. *Journal of Law, Finance, and Accounting*, **2**, 247-275. https://doi.org/10.1561/108.00000022

[5] Pástor, Ľ., Stambaugh, R.F. and Taylor, L.A. (2021) Sustainable Investing in Equilibrium. *Journal of Financial Economics*, **142**, 550-571. https://doi.org/10.1016/j.jfineco.2020.12.011

[6] Pástor, Ľ., Stambaugh, R.F. and Taylor, L.A. (2022) Dissecting Green Returns. *Journal of Financial Economics*, **146**, 403-424. https://doi.org/10.1016/j.jfineco.2022.07.007

[7] Pedersen, L.H., Fitzgibbons, S. and Pomorski, L. (2021) Responsible Investing: The ESG-Efficient Frontier. *Journal of Financial Economics*, **142**, 572-597. https://doi.org/10.1016/j.jfineco.2020.11.001

[8] Engle, R.F., Giglio, S., Kelly, B., Lee, H. and Stroebel, J. (2020) Hedging Climate Change News. *The Review of Financial Studies*, **33**, 1184-1216. https://doi.org/10.1093/rfs/hhz072

[9] Krueger, P., Sautner, Z. and Starks, L.T. (2020) The Importance of Climate Risks for Institutional Investors. *The Review of Financial Studies*, **33**, 1067-1111. https://doi.org/10.1093/rfs/hhz137

[10] Hong, H., Li, F.W. and Xu, J. (2019) Climate Risks and Market Efficiency. *Journal of Econometrics*, **208**, 265-281. https://doi.org/10.1016/j.jeconom.2018.09.015

[11] Ilhan, E., Sautner, Z. and Vilkov, G. (2021) Carbon Tail Risk. *The Review of Financial Studies*, **34**, 1540-1571. https://doi.org/10.1093/rfs/hhaa071

[12] Choi, D., Gao, Z. and Jiang, W. (2020) Attention to Global Warming. *The Review of Financial Studies*, **33**, 1112-1145. https://doi.org/10.1093/rfs/hhz086

[13] Bolton, P. and Kacperczyk, M. (2021) Do Investors Care about Carbon Risk? *Journal of Financial Economics*, **142**, 517-549. https://doi.org/10.1016/j.jfineco.2021.05.008

[14] Giglio, S., Kelly, B. and Stroebel, J. (2021) Climate Finance. *Annual Review of Financial Economics*, **13**, 15-36. https://doi.org/10.1146/annurev-financial-102620-103311

[15] Amihud, Y. (2002) Illiquidity and Stock Returns: Cross-Section and Time-Series Effects. *Journal of Financial Markets*, **5**, 31-56. https://doi.org/10.1016/s1386-4181(01)00024-6

[16] Pástor, Ľ. and Stambaugh, R.F. (2003) Liquidity Risk and Expected Stock Returns. *Journal of Political Economy*, **111**, 642-685. https://doi.org/10.1086/374184

[17] Mendoza, E.G. (2010) Sudden Stops, Financial Crises, and Leverage. *American Economic Review*, **100**, 1941-1966. https://doi.org/10.1257/aer.100.5.1941

[18] Bianchi, J. (2011) Overborrowing and Systemic Externalities in the Business Cycle. *American Economic Review*, **101**, 3400-3426. https://doi.org/10.1257/aer.101.7.3400

[19] Brunnermeier, M.K. (2009) Deciphering the Liquidity and Credit Crunch 2007-2008.

Journal of Economic Perspectives, **23**, 77-100. https://doi.org/10.1257/jep.23.1.77

[20] Brunnermeier, M.K. and Sannikov, Y. (2014) A Macroeconomic Model with a Financial Sector. *American Economic Review*, **104**, 379-421. https://doi.org/10.1257/aer.104.2.379

[21] Adrian, T. and Brunnermeier, M.K. (2016) CoVaR. *American Economic Review*, **106**, 1705-1741. https://doi.org/10.1257/aer.20120555

[22] Stiefenhofer, P. (2016) Production in General Equilibrium with Incomplete Financial Markets. *Journal of Mathematical Finance*, **6**, 293-302. https://doi.org/10.4236/jmf.2016.62025

[23] Stiefenhofer, P. (2017) Existence of Financial Equilibria in a General Equilibrium Model with Piece-Wise Smooth Production Manifolds. *Journal of Mathematical Finance*, **7**, 671-681. https://doi.org/10.4236/jmf.2017.73035

[24] Stiefenhofer, P. and Deniz, C. (2026) Rethinking Firm Behavior When Financial Markets Are Incomplete: A General Equilibrium Model Enhanced by Artificial Intelligence. In: Trinh, V.Q. and Pham, T.N., *The Future of Accounting and Finance*: *Embracing Technology*, *Digitalisation*, *Sustainability*, *Education*, *and Employability*, Springer, 21-40. https://doi.org/10.1007/978-3-032-03943-9_2

[25] Stiefenhofer, P.C. (2010) Corporate Equilibrium Properties of a Centralized Objective Function GEI Model (No. 10/18). 1-8.

[26] Stiefenhofer, P. (2026) A Neurofinance Framework for Subjective Temporal Perception, Risk, and Investment Behavior. arXiv preprint arXiv:2608.14930 [econ.GN]. https://arxiv.org/pdf/2608.14930

[27] Stiefenhofer, P., Deniz, C., Chen, Y., Qian, J. and Almehthel, H.M. (2024) The Future of Sustainable Finance: AI-Driven Sustainable Pairs Trading in Market-Neutral Investing. In: Walker, T., Gramlich, D. and Sadati, A., *Artificial Intelligence*, *Finance*, *and Sustainability*, Springer, 111-142.

[28] Bollen, N.P.B. (2007) Mutual Fund Attributes and Investor Behavior. *Journal of Financial and Quantitative Analysis*, **42**, 683-708. https://doi.org/10.1017/s0022109000004142

[29] Geczy, C.C., Stambaugh, R.F. and Levin, D. (2021) Investing in Socially Responsible Mutual Funds. *The Review of Asset Pricing Studies*, **11**, 309-351. https://doi.org/10.1093/rapstu/raab004

[30] Bauer, R., Koedijk, K. and Otten, R. (2005) International Evidence on Ethical Mutual Fund Performance and Investment Style. *Journal of Banking & Finance*, **29**, 1751-1767. https://doi.org/10.1016/j.jbankfin.2004.06.035

[31] Renneboog, L., Ter Horst, J. and Zhang, C. (2008) Socially Responsible Investments: Institutional Aspects, Performance, and Investor Behavior. *Journal of Banking & Finance*, **32**, 1723-1742. https://doi.org/10.1016/j.jbankfin.2007.12.039

[32] Renneboog, L., Ter Horst, J. and Zhang, C. (2011) Is Ethical Money Financially Smart? Nonfinancial Attributes and Money Flows of Socially Responsible Investment Funds. *Journal of Financial Intermediation*, **20**, 562-588. https://doi.org/10.1016/j.jfi.2010.12.003

[33] Białkowski, J. and Starks, L.T. (2016) SRI Funds: Investor Demand, Exogenous Shocks and ESG Profiles.

[34] Riedl, A. and Smeets, P. (2017) Why Do Investors Hold Socially Responsible Mutual Funds? *The Journal of Finance*, **72**, 2505-2550. https://doi.org/10.1111/jofi.12547

[35] Hartzmark, S.M. and Sussman, A.B. (2019) Do Investors Value Sustainability? A Nat-

ural Experiment Examining Ranking and Fund Flows. *The Journal of Finance*, **74**, 2789-2837. https://doi.org/10.1111/jofi.12841

[36] Baker, M., Bergstresser, D., Serafeim, G. and Wurgler, J. (2018) Financing the Response to Climate Change: The Pricing and Ownership of US Green Bonds (No. w25194). National Bureau of Economic Research.

[37] Zerbib, O.D. (2019) The Effect of Pro-Environmental Preferences on Bond Prices: Evidence from Green Bonds. *Journal of Banking & Finance*, **98**, 39-60. https://doi.org/10.1016/j.jbankfin.2018.10.012

[38] Dyck, A., Lins, K.V., Roth, L. and Wagner, H.F. (2019) Do Institutional Investors Drive Corporate Social Responsibility? International Evidence. *Journal of Financial Economics*, **131**, 693-714. https://doi.org/10.1016/j.jfineco.2018.08.013

[39] Berg, F., Kölbel, J.F. and Rigobon, R. (2022) Aggregate Confusion: The Divergence of ESG Ratings. *Review of Finance*, **26**, 1315-1344. https://doi.org/10.1093/rof/rfac033

[40] Bansal, R., Ochoa, M. and Kiku, D. (2016) Climate Change and Growth Risks. NBER Working Paper No. 23009.

[41] Dimson, E., Karakaş, O. and Li, X. (2015) Active Ownership. *Review of Financial Studies*, **28**, 3225-3268. https://doi.org/10.1093/rfs/hhv044

[42] Chen, J., Hong, H. and Stein, J.C. (2002) Breadth of Ownership and Stock Returns. *Journal of Financial Economics*, **66**, 171-205. https://doi.org/10.1016/s0304-405x(02)00223-4

[43] Gibson Brandon, R., Krueger, P. and Schmidt, P.S. (2021) ESG Rating Disagreement and Stock Returns. *Financial Analysts Journal*, **77**, 104-127. https://doi.org/10.1080/0015198x.2021.1963186

[44] Gavriilidis, K. (2021) Measuring Climate Policy Uncertainty. https://papers.ssrn.com/sol3/papers.cfm?abstract_id=3847388

[45] Hamilton, J.D. (1989) A New Approach to the Economic Analysis of Nonstationary Time Series and the Business Cycle. *Econometrica*, **57**, 357-384. https://doi.org/10.2307/1912559

[46] Hansen, B.E. (2000) Sample Splitting and Threshold Estimation. *Econometrica*, **68**, 575-603. https://doi.org/10.1111/1468-0262.00124

[47] Battiston, S., Mandel, A., Monasterolo, I., Schütze, F. and Visentin, G. (2017) A Climate Stress-Test of the Financial System. *Nature Climate Change*, **7**, 283-288. https://doi.org/10.1038/nclimate3255

Appendix A. Numerical Illustration of the Hybrid Viability Mechanism

The purpose of this appendix is not to calibrate a particular economy, but to verify that the theoretical mechanism developed in the paper is internally operational. In particular, the simulations examine whether valuation equilibrium and viability equilibrium may diverge under the endogenous regime-switching system developed in Section 2. The analysis proceeds by simulating the stochastic hybrid dynamical system generated by the state equations (20), the sustainability-fragility index (30), and the hysteretic switching rule (43).

A.1. Stochastic State Dynamics

Let

$$u(t)=\left(\bar{d}(t),\lambda(t),z(t),q(t),\ell(t),c(t)\right)\in D$$

denote the macro-financial state vector introduced in Equation (17).

The simulated economy evolves according to the stochastic differential system

$$\mathrm{d}u(t)=F_{\sigma(t)}\left(u(t)\right)\mathrm{d}t+\Sigma_{\sigma(t)}^{1/2}\mathrm{d}W(t), \tag{78}$$

where

$$\sigma(t)\in\{G,F\}$$

denotes the prevailing regime,

$$F_{\sigma}$$

is the deterministic vector field defined in Equation (20),

$$W(t)=\left(W_1(t),\cdots,W_6(t)\right)$$

is a six-dimensional standard Wiener process,
and

$$\Sigma_{\sigma}$$

is a positive-definite covariance matrix governing exogenous shocks.

The diffusion term introduces stochastic fluctuations in ESG demand, investor participation, information quality, market liquidity, systemic stress, and climate concern. The Gaussian diffusion is therefore interpreted as the unconstrained innovation before feasibility projection; admissibility is enforced at every numerical update by P_D below.

A.2. Euler-Maruyama Approximation

Equation (78) is approximated using the Euler-Maruyama method.

For a time step

$$\Delta t>0,$$

the state evolves according to

$$u_{t+1}=P_D\left[u_t+F_{\sigma_t}(u_t)\Delta t+\Sigma_{\sigma_t}^{1/2}\sqrt{\Delta t}\,\varepsilon_t\right], \tag{79}$$

where

$$\varepsilon_t \sim N(0, I_6)$$

independently across periods. The projection P_D is the coordinatewise Euclidean projection onto the admissible state space D: non-negative coordinates are truncated at zero and the bounded coordinates λ, q, and ℓ are projected onto $[0,1]$. Consequently every simulated state remains in D despite the unbounded support of the Gaussian innovation. This is the discrete-time counterpart of the projected deterministic dynamics in Equation (22).

Throughout the simulations, we set

$$\Delta t = 0.01.$$

A.3. Endogenous Regime Selection

At each time step, the sustainability-fragility index

$$\Xi(u_t)$$

is computed from Equation (30).

The prevailing regime is then updated according to the hysteretic switching rule

$$\sigma_{t+1} = \begin{cases} F, & \Xi(u_t) \geq \overline{\zeta}_+, \\ G, & \Xi(u_t) \leq \overline{\zeta}_-, \\ \sigma_t, & \overline{\zeta}_- < \Xi(u_t) < \overline{\zeta}_+. \end{cases} \tag{80}$$

This construction generates a stochastic hybrid dynamical system combining continuous state evolution with discrete regime changes.

A.4. Monte Carlo Design

The simulation consists of

$$M = 10000$$

independent sample paths.

Each path is simulated over

$$T = 500$$

periods.

Initial states are sampled from a uniform distribution over the admissible state space

$$D.$$

For every path and every period, we record

$$u_t, \quad \sigma_t, \quad \Xi(u_t), \quad B_G(u_t), \quad B_F(u_t), \quad \mu_{g,t}.$$

The greenium is computed using Equation (15).

A.5. Numerical Illustration Criteria

The numerical exercise illustrates three implications of the theory within the model-generated environment. It is not an empirical validation exercise: the states,

transition labels, and viability frontiers are generated by the same imposed dynamics and thresholds.

First, we illustrate the equilibrium-viability separation established in Theorem 1. Specifically, we identify simulated states satisfying

$$F_\sigma\left(u^*\right)=0$$

and compare them with the history-consistent continuation conditions. An active growth-regime equilibrium is incompatible when

$$\Xi\left(u_G^*\right)\geq \overline{\zeta}_+,$$

whereas an active fragility-regime equilibrium is incompatible when

$$\Xi\left(u_F^*\right)\leq \overline{\zeta}_-.$$

Thus the exercise illustrates, rather than independently tests, the separation between frozen-regime equilibrium and hybrid-regime compatibility.

Second, we illustrate the greenium non-identification result established in Corollary 1. Pairs of states are identified such that

$$\mu_g(u)=\mu_g(v),$$

while

$$u\in\mathcal{C}_\sigma,\quad v\notin\mathcal{C}_\sigma.$$

Third, we examine whether the viability margins

$$B_G(u)=\overline{\zeta}_+-\Xi(u)$$

and

$$B_F(u)=\Xi(u)-\overline{\zeta}_-$$

classify model-generated future regime transitions differently from valuation measures alone.

A.6. Transition-Risk Classification

Define

$$Y_t=1$$

if a regime transition occurs within the next h periods and

$$Y_t=0$$

otherwise.

We estimate

$$\Pr\left(Y_t=1\right)=\Lambda\left(\alpha+\beta_1\mu_{g,t}\right), \tag{81}$$

and compare it with

$$\Pr\left(Y_t=1\right)=\Lambda\left(\alpha+\beta_1 B_t\right), \tag{82}$$

where

$$B_t=B_G\left(u_t\right)$$

or

$$B_t = B_F(u_t).$$

Classification accuracy, pseudo- R^2, area under the ROC curve, and out-of-sample prediction errors are reported.

Because the transition labels are generated from the imposed state dynamics and switching thresholds, these comparisons are interpreted only as numerical diagnostics of how alternative reduced-form classifiers recover the model-generated transition mechanism; they do not establish empirical forecasting power.

B. Stochastic Hybrid Simulation: Reproducibility and Numerical Evidence

This appendix reports the full reproducibility record and the numerical outputs from the stochastic hybrid simulation used to illustrate the distinction between valuation-based greenium effects and equilibrium viability. The simulation implements the six-dimensional state vector $\left(\bar{d}_t, \lambda_t, z_t, q_t, \ell_t, c_t\right)$, constructs the sustainability-fragility index $\Xi\left(u_t\right)$, applies the two-threshold switching rule $\left(\underline{\zeta}_-, \underline{\zeta}_+\right)$, and evaluates whether observed valuation premia classify future transitions. The evidence is deliberately reported in black-and-white, with fixed seed, fixed sample sizes, and exported tables to make the appendix fully reproducible.

Table A1. Reproducibility record for the stochastic hybrid simulation.

Item	Value	Implementation detail
Random seed	20260614	numpy.random.default_rng seed used for all simulation and sampling draws
Monte Carlo paths	3000	Number of simulated trajectories
Periods per path	500	Discrete periods stored per trajectory
Panel observations	1,500,000	Cartesian path-time panel after simulation
Euler-Maruyama step	0.01	Time step used in stochastic state update
State dimension	6	State vector: dbar, lambda, z, q, ell, c
Prediction horizon	25	Future transition indicator equals one if a regime switch occurs within h periods
Switching thresholds	0.58; 0.92	Recovery threshold zeta_minus and fragility threshold zeta_plus
Initial conditions	Uniform draws	dbar0 in [0.35, 0.90]; lambda0 in [0.25, 0.85]; z0 in [0.10, 0.70]; q0 in [0.35, 0.90]; ell0 in [0.30, 0.90]; c0 in [0.15, 0.85]
Out-of-sample split	65/35	Train-test split with stratification on the transition indicator
Coefficient sample	50,000	Random subsample used for GLM/logit coefficient estimation
Prediction sample	100,000	Random subsample used for out-of-sample classification performance
Robustness sample	10,000 per threshold pair	Random subsample used for threshold-robustness checks
Classification estimator	Logistic regression	StandardScaler followed by LogisticRegression (max_iter = 1000)
Coefficient estimator	Binomial GLM	Statsmodels GLM with logit link; constant and exact collinear regressors removed
Figure format	PDF and PNG	All figures saved as 600 dpi black-and-white outputs

Notes: The table records all computational parameters needed to reproduce the notebook output.

Table A2. Core simulation and economic parameters.

Parameter	Value	Interpretation
M	3000	Monte Carlo paths
T	500	Periods per path
Delta t	0.0100	Euler-Maruyama step size

Continued

h	25.0000	Transition prediction horizon
vartheta	0.8500	Weight on ESG information deterioration
upsilon	0.8500	Weight on green-market illiquidity
rho_d	0.7000	Weight on ESG demand resilience
rho_lambda	0.5500	Weight on participation resilience
rho_c	0.7500	Weight on climate concern
zeta_minus	0.5800	Recovery threshold
zeta_plus	0.9200	Fragility threshold
a	4.0000	Risk aversion
g_g	1.0000	ESG exposure of ESG portfolio

Notes: Parameters correspond to the notebook object extttparam_table.

Table A3. Regime-specific drift and diffusion calibration.

Viable regime (G)		Fragile regime (F)	
(r) 1 - 2 (l) 3 - 4 Parameter	Value	Parameter	Value
ρ	1.2000	ρ	0.8000
$d^{\star}$	0.8200	$d^{\star}$	0.5500
ρ_z	0.1800	ρ_z	0.3500
ρ_q	0.2000	ρ_q	0.0800
Γ	1.0500	Γ	1.4500
κ	1.0000	κ	0.5500
η_d	0.2000	η_d	0.0600
η_λ	0.2000	η_λ	0.0600
η_q	0.2000	η_q	0.0500
ω	0.2000	ω	0.3800
r	1.2500	r	0.7500
$\bar{q}$	0.8200	$\bar{q}$	0.4800
χ	0.1200	χ	0.2500
s	1.1000	s	0.7000
$\bar{\ell}$	0.7800	$\bar{\ell}$	0.4200
ν	0.1500	ν	0.2800
τ	0.1800	τ	0.0600
m	0.9000	m	0.6500
$\bar{c}$	0.3500	$\bar{c}$	0.7800
ξ	0.1400	ξ	0.2800
σ	$(0.050, 0.035, 0.055, 0.035, 0.040, 0.050)$	σ	$(0.065, 0.050, 0.085, 0.055, 0.060, 0.075)$

Notes: The vector σ reports the six componentwise diffusion scales in the order $(\bar{d}, \lambda, z, q, \ell, c)$. The viable regime is characterized by stronger ESG demand, participation, liquidity, and resilience parameters, whereas the fragile regime exhibits higher stress amplification and larger diffusion intensities.

The descriptive statistics in Table A4 show that the simulated panel spans both low-fragility and high-fragility states. The viability margin $B_G = \overline{\zeta}_+ - \Xi$ and fragility margin $B_F = \Xi - \overline{\zeta}_-$ are not transformations of the greenium alone, which is why the same valuation premium can be associated with different viability classifications.

Table A4. Descriptive statistics for the simulated panel.

Variable	N	Mean	SD	Min	P1	P5	P25	Median	P75	P95	P99	Max
dbar	1500000.0000	0.7747	0.1495	0.2532	0.3972	0.4769	0.6659	0.8441	0.8811	0.9206	0.9446	1.0177
lambda	1500000.0000	0.7988	0.1987	0.0046	0.2678	0.3854	0.6780	0.8758	0.9606	0.9943	1.0000	1.0000
z	1500000.0000	0.3553	0.1685	0.0000	0.0000	0.0077	0.2777	0.4184	0.4759	0.5347	0.5824	0.7214
q	1500000.0000	0.6918	0.1378	0.2234	0.3567	0.4108	0.6246	0.7580	0.7836	0.8143	0.8424	0.9112
ell	1500000.0000	0.7299	0.1804	0.1993	0.3142	0.3781	0.6051	0.8190	0.8614	0.8980	0.9195	0.9819
c	1500000.0000	0.5043	0.1676	0.1360	0.2461	0.3254	0.3956	0.4407	0.5740	0.8482	0.9195	1.0781
Xi	1500000.0000	0.2434	0.4187	−0.4619	−0.1884	−0.1353	−0.0513	0.0355	0.4998	1.1068	1.3408	1.7420
greenium	1500000.0000	−0.1937	0.0374	−0.2544	−0.2361	−0.2302	−0.2203	−0.2110	−0.1665	−0.1192	−0.0993	−0.0633
BG	1500000.0000	0.6766	0.4187	−0.8220	−0.4208	−0.1868	0.4202	0.8845	0.9713	1.0553	1.1084	1.3819
BF	1500000.0000	−0.3366	0.4187	−1.0419	−0.7684	−0.7153	−0.6313	−0.5445	−0.0802	0.5268	0.7608	1.1620

Notes: The full panel has 3000*imes*500 = 1,500,000 path-time observations.

Table A5. Regime composition and transition incidence.

regime	observations	mean_Xi	mean_greenium	transition_rate_h	mean_dbar	mean_lambda	mean_z	mean_q	mean_ell	mean_c	share
F	333049	0.9464	−0.1344	0.0226	0.5376	0.5719	0.1185	0.4620	0.4328	0.7725	0.2220
G	1166951	0.0428	−0.2106	0.0000	0.8424	0.8635	0.4229	0.7574	0.8147	0.4277	0.7780

Notes: Regime *G* denotes the viable/green regime and regime *F* denotes the fragile regime.

Table A6. Greenium non-identification pairs.

Pair	Classification	Path	Time	Greenium	Xi	BG	Regime	dbar	lambda	z	q	ell	c
1	Viable	2652	29	−0.2137	−0.3133	1.2333	G	0.8546	0.8544	0.2464	0.8382	0.7651	0.2283
1	Non-viable	2621	10	−0.2137	1.1252	−0.2052	F	0.8546	0.4840	0.4619	0.5482	0.3275	0.7628
2	Viable	1432	276	−0.2145	−0.2154	1.1354	G	0.8581	0.9774	0.4194	0.7905	0.9284	0.3528
2	Non-viable	2169	4	−0.2145	1.2791	−0.3591	F	0.8581	0.4745	0.5764	0.4297	0.4039	0.7638
3	Viable	2468	128	−0.2091	−0.2543	1.1743	G	0.8363	0.9727	0.3480	0.7782	0.8884	0.3130
3	Non-viable	979	10	−0.2091	1.1317	−0.2117	F	0.8363	0.3664	0.5541	0.3926	0.7437	0.8405
4	Viable	782	21	−0.2063	−0.2047	1.1247	G	0.8254	0.7809	0.2915	0.7683	0.8492	0.2480
4	Non-viable	1212	11	−0.2063	1.0060	−0.0860	F	0.8254	0.4968	0.2664	0.4437	0.4052	0.8162
5	Viable	2623	12	−0.1176	0.1006	0.8194	G	0.4703	0.6923	0.1509	0.8286	0.5971	0.2287
5	Non-viable	1587	71	−0.1176	1.5744	−0.6544	F	0.4703	0.3477	0.5200	0.3042	0.4089	0.6413

Notes: Each pair reports one viable and one non-viable observation with nearly identical greenium.

Table A6 gives the central non-identification check. Within extremely narrow greenium bins, observations can have virtually identical greenium values while lying on opposite sides of the viability boundary. Hence the greenium is informative about one valuation component but does not identify equilibrium viability.

Table A7. Greenium difference tests across viability classes.

Test	Null	Statistic	p_value	Mean_viable	Mean_nonviable
Welch t-test	Equal mean greenium across G-viability classes	−234.0686	0.0000	−0.2008	−0.1283
Mann-Whitney U	Equal greenium distributions across G-viability classes	21093760.0000	0.0000	−0.2008	−0.1283

Notes: Tests are computed on every twenty-fifth observation to reduce mechanical serial dependence in the very large simulated panel.

Table A8. Logit coefficient estimates for transition prediction.

Model	Variable	Coefficient	Std_Error	z_stat	p_value
Valuation only	const	−0.9243	0.2411	−3.8335	0.0001
Valuation only	greenium	25.6756	1.5686	16.3688	0.0000
Viability margin	const	−4.4845	0.0739	−60.6687	0.0000
Viability margin	BG	−1.7196	0.1286	−13.3732	0.0000
Full state	const	−10.4006	1.1960	−8.6963	0.0000
Full state	dbar	5.9807	1.1449	5.2238	0.0000
Full state	lambda	8.9581	0.6079	14.7351	0.0000
Full state	z	−34.5495	2.8393	−12.1682	0.0000
Full state	q	1.8226	1.2444	1.4647	0.1430
Full state	ell	0.5632	1.2072	0.4665	0.6408
Full state	c	−4.2439	0.8755	−4.8476	0.0000
Full state + greenium	const	−10.4006	1.1960	−8.6963	0.0000
Full state + greenium	dbar	5.9807	1.1449	5.2238	0.0000
Full state + greenium	lambda	8.9581	0.6079	14.7351	0.0000
Full state + greenium	z	−34.5495	2.8393	−12.1682	0.0000
Full state + greenium	q	1.8226	1.2444	1.4647	0.1430
Full state + greenium	ell	0.5632	1.2072	0.4665	0.6408
Full state + greenium	c	−4.2439	0.8755	−4.8476	0.0000

Notes: The dependent variable equals one if a regime transition occurs within horizon $h = 25$. Exact collinear variables are removed in the GLM coefficient estimation.

Table A9. Out-of-sample transition-risk classification performance.

Model	AUC	Accuracy	Brier	LogLoss
Full state	0.9780	0.9951	0.0045	0.0177
Full state + greenium	0.9779	0.9951	0.0045	0.0178
Valuation only	0.8261	0.9951	0.0049	0.0280
Viability margin	0.7761	0.9951	0.0049	0.0294

Notes: Models are trained on 65 percent and evaluated on 35 percent of a stratified random sample of 100,000 observations.

Table A10. Robustness to alternative switching thresholds.

zeta_minus	zeta_plus	Model	AUC	Brier	Share_viable_G
0.5200	0.8600	Greenium	0.8234	0.0045	0.8585
0.5200	0.8600	Alt viability margin	0.7841	0.0045	0.8585
0.5500	0.8900	Greenium	0.8234	0.0045	0.8714
0.5500	0.8900	Alt viability margin	0.7841	0.0045	0.8714
0.5800	0.9200	Greenium	0.8234	0.0045	0.8838
0.5800	0.9200	Alt viability margin	0.7841	0.0045	0.8838
0.6100	0.9500	Greenium	0.8234	0.0045	0.8970
0.6100	0.9500	Alt viability margin	0.7841	0.0045	0.8970
0.6400	0.9800	Greenium	0.8234	0.0045	0.9083
0.6400	0.9800	Alt viability margin	0.7841	0.0045	0.9083

Notes: The baseline threshold pair is (0.58, 0.92). Within the model-generated sample, the full-state classifier recovers the imposed transition mechanism more accurately than the valuation-only classifier. This is a numerical illustration rather than empirical evidence of forecasting power. It is consistent with the theoretical distinction between a market greenium, which is a valuation implication, and viability, which is a state-contingent property of the hybrid dynamic system.

Appendix Figures

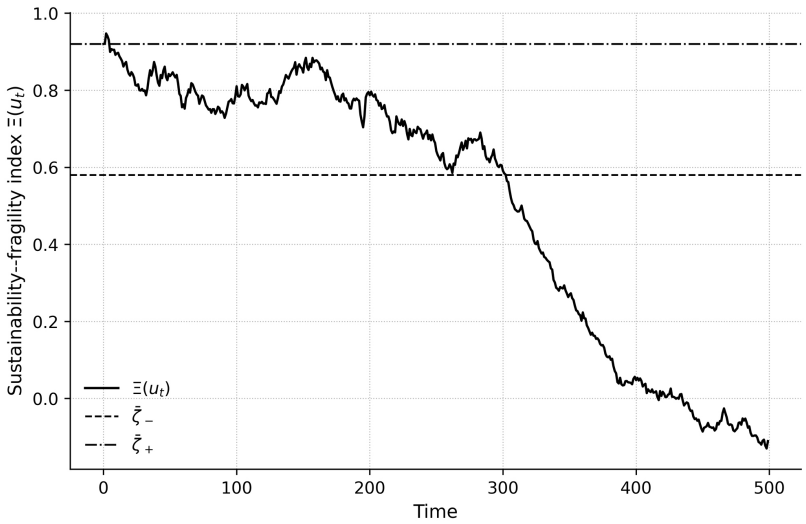

Figure A1. Sustainability-fragility index along a representative simulated path. The dashed and dash-dotted horizontal lines report $\bar{\zeta}_-$ and $\bar{\zeta}_+$.

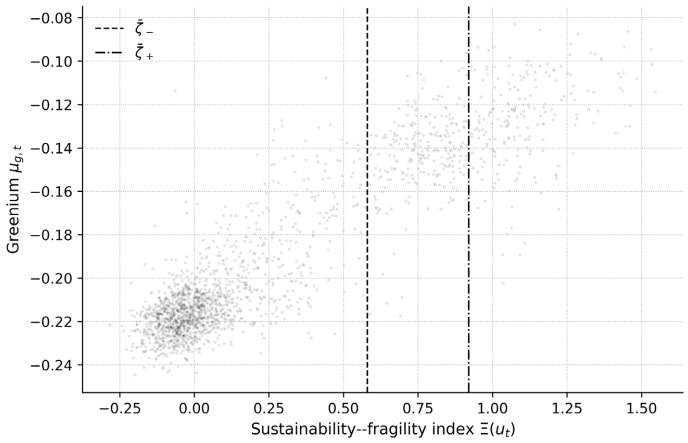

Figure A2. Greenium and viability are not equivalent. The same greenium range contains observations on both sides of the viability thresholds.

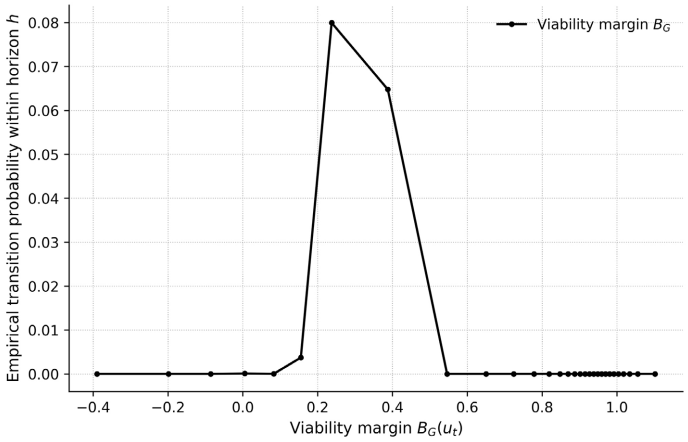

Figure A3. Model-generated transition frequency by growth-regime continuation margin $B_G(u_t)$. Larger continuation margins are associated with lower transition incidence in the simulated environment.

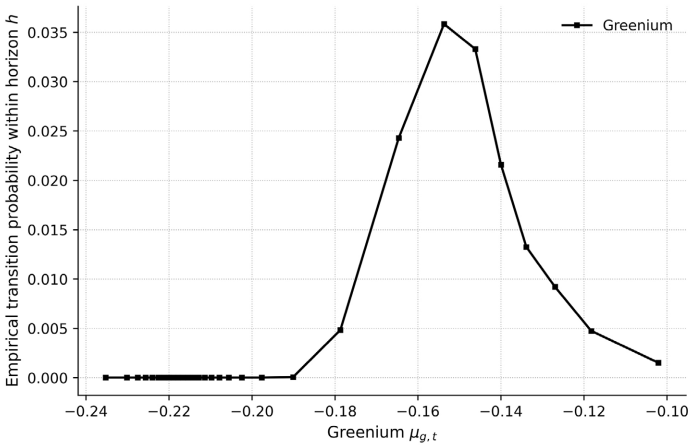

Figure A4. Model-generated transition frequency by greenium. Within the simulated environment, the greenium is an imperfect classifier of transitions generated by the imposed hybrid dynamics.

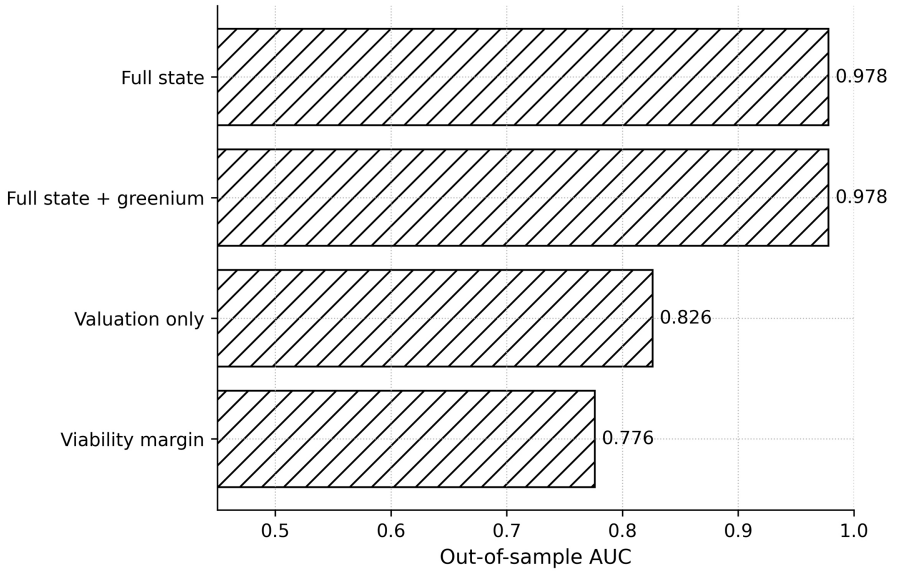

Figure A5. Hold-out-sample AUC within the model-generated data. State-based classifiers recover the imposed transition mechanism more accurately than valuation-only specifications; this is not an empirical forecasting exercise.

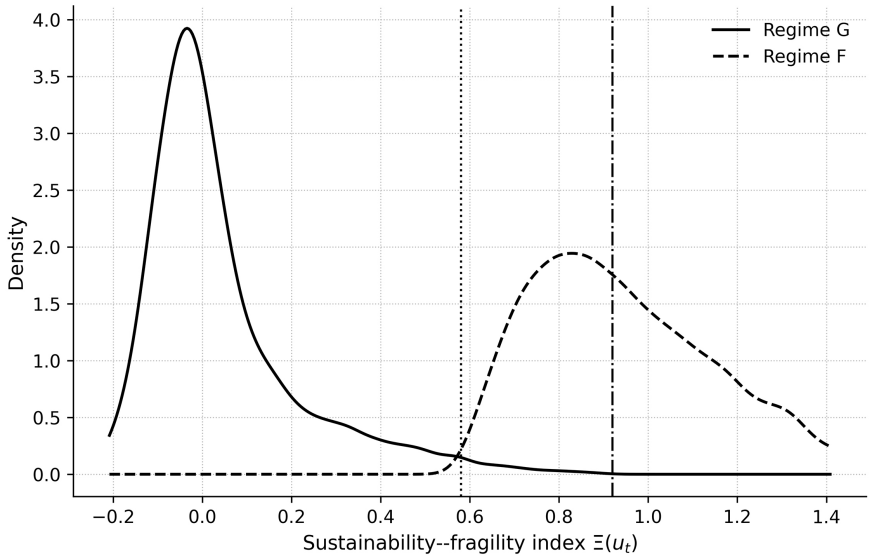

Figure A6. Distribution of the sustainability-fragility index by regime. The threshold structure separates the low-fragility and high-fragility state regions while allowing hysteresis between the two boundaries.

Jointly, **Figures A1-A6** visually summarize the model-generated patterns reported in the appendix tables. The model generates persistent low- and high-fragility regimes, displays transition risk as a function of state-space distance from the viability boundary, and shows that valuation premia alone do not recover the dynamic viability classification.

The numerical results in this appendix are generated from the model itself. They demonstrate internal operation, reproducibility, and the distinction among valuation,

regime compatibility, and transition geometry under the stated parameterization. They should not be interpreted as external empirical validation, causal evidence, or evidence of real-world forecasting performance.